

# Structure of the Dimeric Ethylene Glycol–Vanadate Complex and Other 1,2-Diol–Vanadate Complexes in Aqueous Solution: Vanadate-Based Transition-State Analog Complexes of Phosphotransferases<sup>1</sup>

W. J. Ray, Jr.,<sup>\*,†</sup> D. C. Crans,<sup>\*,‡</sup> J. Zheng,<sup>§</sup> J. W. Burgner, II,<sup>§</sup> H. Deng,<sup>§</sup> and M. Mahroof-Tahir<sup>‡</sup>

Contribution from the Department of Biological Sciences, Purdue University, West Lafayette, Indiana 47907, Department of Chemistry, Colorado State University, Fort Collins, Colorado 80523-1872, and Department of Physics, City College of the City University of New York, New York 10031

Received November 7, 1994<sup>®</sup>

**Abstract:** The solution structure of the complex produced by the condensation of 2 mol of vanadate with 2 mol of a vicinal diol in aqueous solution has been characterized. This characterization is based on an assessment of the effect of water on the equilibrium constant for formation of the dimeric ethylene glycol–vanadate complex at high and intermediate ethylene glycol concentrations, on <sup>51</sup>V, <sup>13</sup>C, <sup>1</sup>H, and <sup>17</sup>O NMR studies, and on an evaluation of the vibrational frequency of the VO stretching mode for non-ester oxygens in the natural abundance and <sup>18</sup>O-labeled dimers, using Raman difference spectroscopy and Fourier transform infrared difference spectroscopy. The solution structure is analogous to that previously reported in the solid state for the related dimeric vanadium complexes of 2-ethyl-2-hydroxybutyric acid and of pinacol. That structure contains a four-membered V<sub>2</sub>O<sub>2</sub> unit within the framework of two VO<sub>5</sub> clusters that each are part of a five-membered ring involving the diol. The vibrational properties of the VO<sub>5</sub> cluster in the dimeric ethylene glycol–vanadate complex are compared with those in dimers produced by the condensation of vanadate with  $\alpha$ -hydroxy acids and of VOCl<sub>3</sub> with ethylene glycol and pinacol. <sup>1</sup>H and <sup>13</sup>C NMR studies are used to investigate the interconversion of isomeric forms of two dimeric 1,2-diol–vanadate complexes and one dimeric  $\alpha$ -hydroxy acid–vanadate complex. Several conclusions can be drawn about the structures of five-coordinate vanadates and vanadate-based transition-state analog complexes with phosphotransferases on the basis of the proposed structure for these complexes.

## Introduction

The potent inhibition of ribonuclease A<sup>2</sup> by a 1:1 complex of uridine and vanadate has elicited considerable interest in the structure of the major uridine–vanadate complex in solution because of its presumed relationship to the transition state for phosphoryl transfer reactions. So far, four different structures have been proposed for the major 2:2 uridine–vanadate complex (Figure 1).<sup>3–13</sup> Structural information on the solution species of this and related vanadate–diol complexes thus can be used

to provide mechanistic information for phosphotransferases.<sup>14,15</sup> Although the structures of three vanadium (5+) complexes with diol or  $\alpha$ -hydroxycarboxylic acid ligands have been determined by X-ray crystallography,<sup>12,15,16</sup> characterization of the solution structure is particularly desirable since solution and solid-state structures may not be identical.<sup>17</sup> Indeed, the vanadium atoms in the solid states of these three derivatives are five coordinate in contrast to the more common vanadium(V) complexes, where the vanadium atom, in the form of a VO<sub>2</sub><sup>+</sup> unit, is octahedral.<sup>18</sup> Whether all vanadium(V) complexes with vicinal diols and  $\alpha$ -hydroxycarboxylic acids are five coordinate in aqueous solution remains to be determined. The present paper provides

<sup>†</sup> Purdue University.

<sup>‡</sup> Colorado State University.

<sup>§</sup> City College of the City University of New York.

<sup>®</sup> Abstract published in *Advance ACS Abstracts*, April 1, 1995.

(1) Abbreviations and symbols are as follows: (–V)<sub>2</sub>, the dimeric vanadate complex formed by condensation of 2 mol of vanadate with 2 mol of the entity that appears in the designated blank; *a*, activity;  $\beta$ MR,  $\beta$ -methyl riboside; EG, ethylene glycol; EHB, 2-ethyl-2-hydroxybutanoic acid; FTIR, Fourier-transform infrared (spectroscopy); HiB, 2-hydroxy-isobutyric acid; MCD, magnetic circular dichroism; NMR, nuclear magnetic resonance; (P/VCl)<sub>2</sub>, the dimeric complex formed by condensation of 2 mol each of pinacol, P, and VOCl<sub>3</sub> under anhydrous conditions;<sup>31</sup> U, uridine; V<sub>*i*</sub>, vanadate; *vu*, valence units;<sup>25</sup>  $\cdot\cdot$ , as in terminal VO<sub>2</sub> atom–atom connectivity with multiple bond character;  $\cdot\cdot$ , as in bridging VO<sub>2</sub>–VO<sub>2</sub> atom–atom connectivity with substantially less than single bond character.

(2) Lindquist, R. N.; Lynn, J. L., Jr.; Lienhard, G. E. *J. Am. Chem. Soc.* **1973**, *95*, 8762–8768.

(3) Gresser, M. J.; Tracey, A. S. *J. Am. Chem. Soc.* **1986**, *108*, 1935–1939.

(4) Tracey, A. S.; Gresser, M. J.; Liu, S. *J. Am. Chem. Soc.* **1988**, *110*, 5869–5874.

(5) Tracey, A. S.; Gresser, M. J. *Inorg. Chem.* **1988**, *27*, 2695–2702.

(6) Tracey, A. S.; Jaswal, J. S.; Gresser, M. J.; Rehder, D. *Inorg. Chem.* **1990**, *29*, 4283–4288.

(7) Galdes, C. F. G. C.; Castro, M. M. C. A. *J. Inorg. Biochem.* **1989**, *35*, 79–93.

(8) Galdes, C. F. G. C.; Castro, M. M. C. A. *J. Inorg. Biochem.* **1989**, *37*, 213–232.

(9) Rehder, D.; Holst, H.; Quaas, R.; Hinrichs, W.; Hahn, U.; Saenger, W. *J. Inorg. Biochem.* **1989**, *37*, 141–150.

(10) Tracey, A. S.; Leon-Lai, C. H. *Inorg. Chem.* **1991**, *30*, 3200–3204.

(11) Zhang, X.; Tracey, A. S. *Acta Chem. Scand.* **1992**, *46*, 1170–1176.

(12) Crans, D. C.; Harnung, S. E.; Larsen, E.; Shin, P. K.; Theisen, L. A.; Trajberg, I. *Acta Chem. Scand.* **1991**, *45*, 456–462.

(13) Harnung, S. E.; Larsen, E.; Pedersen, E. J. *Acta Chem. Scand.* **1993**, *47*, 674–682.

(14) Deng, H.; Ray, W. J., Jr.; Burgner, J. W., II; Callender, R. *Biochemistry* **1993**, *32*, 12984–12992.

(15) Richter, J.; Rehder, D. *Z. Naturforsch.* **1991**, *46b*, 1613–1620.

(16) Hambley, T. W.; Judd, R. J.; Lay, P. A. *Inorg. Chem.* **1992**, *31*, 343–345.

(17) Crans, D. C.; Chen, H.; Anderson, O. P.; Miller, M. M. *J. Am. Chem. Soc.* **1993**, *115*, 6769–6776 (see also ref 32).

(18) Scheidt, W. R.; Collins, D. M.; Hoard, J. L. *J. Am. Chem. Soc.* **1971**, *93*, 3873–3877.

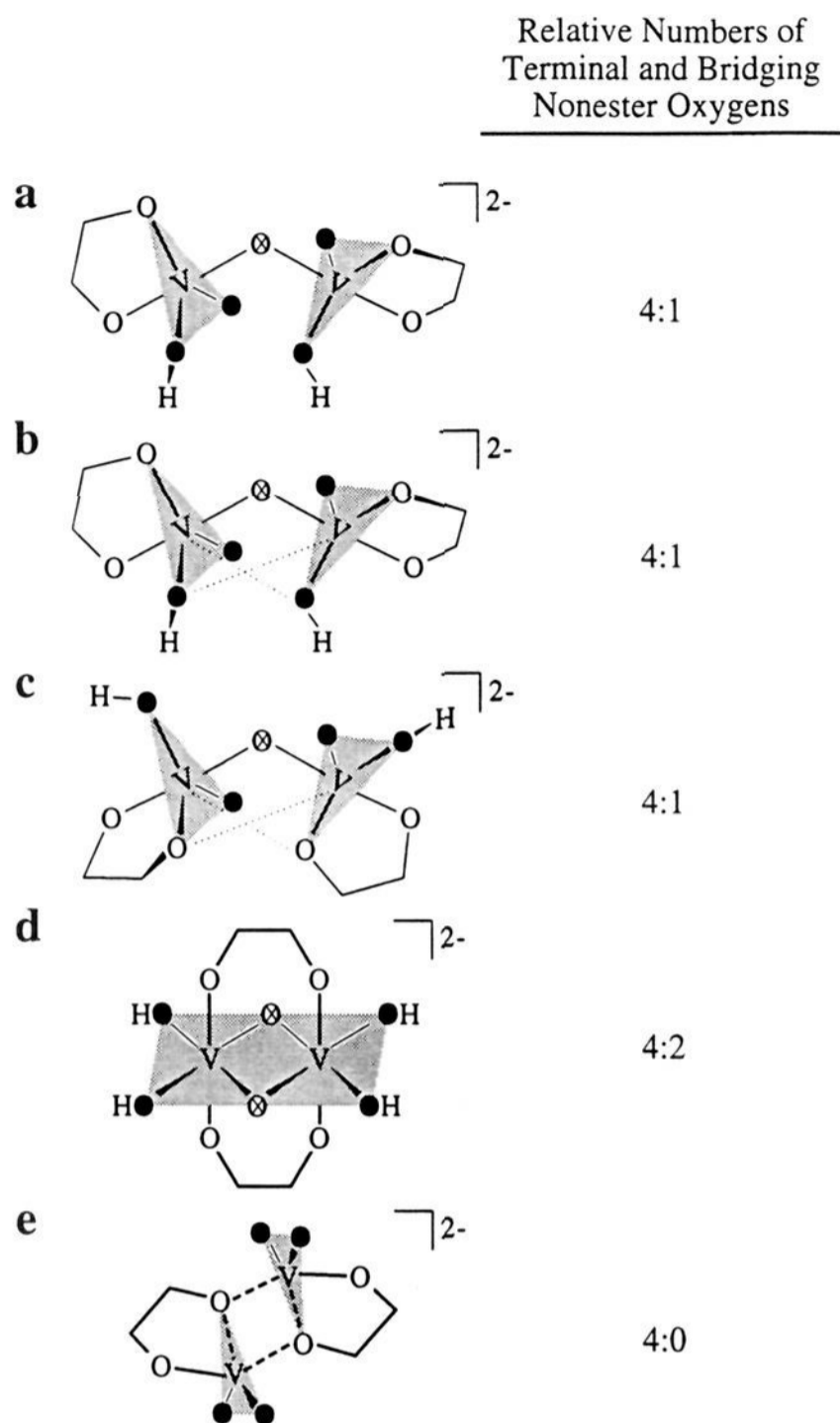


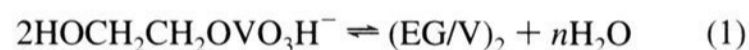
**Figure 1.** Proposed structures for the dimeric ethylene glycol–vanadate complex ((EG/V)<sub>2</sub>): (a) initial proposal of Gresser and Tracey;<sup>3</sup> (b) conformationally restricted structure proposed by Tracey and Leon-Lai;<sup>10</sup> (c) conformationally restricted structure proposed by Richter and Rehder;<sup>15</sup> (d) proposal of Crans *et al.*;<sup>31</sup> (e) structure proposed in this work. The right-hand column indicates the relative numbers of nonbridging oxygen atoms (●) and bridging oxygen atoms (⊗) that are expected to produce different <sup>17</sup>O NMR signals. Dotted (···) and broken (---) lines indicate weak covalent bonds, and the shaded area shows the plane that contains the vanadium and selected oxygen atoms.

structural information that settles this question for the vanadate esters of a series of vicinal diols and leads directly to the solution structures of the related vanadate esters of nucleotides.

The first study of vanadate complexes with an aliphatic diol involved the simplest glycol, ethylene glycol,<sup>3</sup> and showed that, in aqueous solution, the major product is a cyclic diester dimer with a 2:2 stoichiometry ((EG/V)<sub>2</sub>). (The 1:1 complex, if present, is only a minor component of the equilibrium mixture and thus would be difficult to detect.) The first study, and several subsequent studies, provided formation constants for several different 1,2-diol–vanadate complexes ((diol/V)<sub>2</sub>), mostly based on analysis of equilibrium mixtures produced by different concentrations of reactants using <sup>51</sup>V NMR spectroscopy.<sup>3–13</sup> The structure proposed by Gresser and Tracey for the dimeric ethylene glycol complex ((EG/V)<sub>2</sub>) based on this first study contains five-coordinate vanadium (Figure 1a).<sup>3</sup> Later, conformational restrictions, based on <sup>1</sup>H NMR and UV spectroscopic studies of mixtures of vanadate and nucleosides (Figure 1b), were accommodated by Tracey and Leon-Lai, by proposing additional interaction of an oxygen atom and the

vanadium atom.<sup>10</sup> Subsequently, a variant of this conformationally rigid structure was suggested by Richter and Rehder<sup>15</sup> on the basis of the structural precedence for bridging alkoxide ligands (Figure 1c). Crans *et al.*<sup>12</sup> later suggested a structure wherein the vanadium atom is six coordinate (Figure 1d) on the basis of MCD studies of several nucleoside–vanadate dimers. Support for the latter structure was provided by Harnung *et al.*<sup>13</sup> on the basis of MCD studies of vanadate solutions and <sup>1</sup>H and <sup>13</sup>C NMR studies of α-hydroxycarboxylic acid–vanadate systems. At present, none of the proposed structures is consistent with all known experimental data accumulated for solution complexes. Hence, experimental approaches that can provide new structural insight are in order.

Part of the difficulty in characterizing the solution structure of (diol/V)<sub>2</sub> arises because the equilibrium mixtures of reactants and products yield spectra with overlapping signals that require extrapolation for analysis and characterization of properties of the complexes present in solution. Furthermore, the presence of buffers can alter the proportions of most species in these mixtures and complicate the analysis by increasing line widths; this problem becomes particularly critical when solutions contain little water.<sup>19,20</sup> We chose both the system and conditions so that essentially all of the vanadium(V) in the solution was present as the desired 2:2 dimeric complex and used no buffer in these studies. Vicinal diols that formed stronger complexes with vanadate were amenable to study in dilute aqueous solutions and were used to explore specific characteristics of these complexes. Our results lead to a new structural proposal for (diol/V)<sub>2</sub> (Figure 1e) that combines features of all the four previously proposed structures. However, none of these earlier proposals contain the four-membered V<sub>2</sub>O<sub>2</sub> unit within the ten-membered ring proposed here. The structure shown in Figure 1e emerged after re-evaluating the previously proposed stoichiometry, using activities in place of concentrations, and showing that *n* in eq 1 is 2, not 1. Characterization of the



complex by Raman spectroscopy and structural precedences for related 2:2 complexes in the solid state<sup>12,15,16</sup> also played a role in defining this structure. The observation of a 1:1 vanadate–uridine complex bound to ribonuclease provided precedence of a vanadium(V)–diol in aqueous solution containing five-coordinate vanadium.<sup>2,21,22</sup> This paper describes an extensive examination of the new structural proposal (Figure 1e) which correlates all of the data related to these complexes.

## Experimental Section

**General Procedure.** Commercial anhydrous ethylene glycol (Fluka) was dispensed under N<sub>2</sub> and used without further drying. In view of the high concentration of ethylene glycol and the low concentrations of H<sub>2</sub>O frequently used herein, ethylene glycol–water concentrations usually are expressed in percent (v/v). A 1.00 M stock solution of NaH<sub>2</sub>VO<sub>4</sub> was produced by stirring NaVO<sub>3</sub> (Aldrich) with 0.01 equiv of aqueous NaOH at 60 °C until the solid dissolved. Stock solutions of LiH<sub>2</sub>VO<sub>4</sub> (1.88 M), (CH<sub>3</sub>)<sub>4</sub>NH<sub>2</sub>VO<sub>4</sub> (1.70 M), and (*n*-Bu)<sub>4</sub>NH<sub>2</sub>VO<sub>4</sub> (1.40 M) were prepared by stirring V<sub>2</sub>O<sub>5</sub> (Aldrich) overnight with 2 equiv of aqueous 2 N LiOH, methanolic 1.78 N (CH<sub>3</sub>)<sub>4</sub>NOH (Aldrich), or methanolic 1.44 N (*n*-Bu)<sub>4</sub>NOH (Aldrich). If the solution was noticeably yellow, 1–2% more base was added, which, on standing, eliminated the strong yellow color. Undissolved material was removed

(19) Crans, D. C.; Schelble, S. M.; Theisen, L. A. *J. Org. Chem.* **1991**, *56*, 1266–1274.

(20) Crans, D. C. *Comments Inorg. Chem.* **1994**, *16*, 1–33.

(21) Alber, T.; Gilbert, W. A.; Ponzi, D. R.; Petsko, G. A. *Ciba Found. Symp.* **1983**, *93*, 4–24.

(22) Wlodawer, A.; Miller, M.; Sjölin, L. *Proc. Natl. Acad. Sci. U.S.A.* **1983**, *80*, 3628–3631.

by centrifugation, and the vanadate present was quantified by comparison with the UV absorbances for a standard 1.00 M  $\text{NaH}_2\text{VO}_4$  solution prepared from  $\text{NaVO}_3$  (Aldrich) and diluted  $10^4$ -fold in 2 N NaOH. When needed,  $\text{H}_2\text{VO}_4^-$  salts (without water of hydration) were obtained by evaporating these solutions to dryness under vacuum (protected from direct light).  $[\text{^{18}O}]\text{H}_2\text{O}$  (99%, Isotec) was condensed in a cold trap to reduce metal ion contamination before addition to the vanadate salts. A dry solid containing  $^{18}\text{O}$ -labeled vanadate was obtained by successively dissolving a dried  $\text{H}_2\text{VO}_4^-$  salt in a large excess of  $[\text{^{18}O}]\text{H}_2\text{O}$ , followed by rotary evaporation. A solution of  $(\text{CH}_3\text{O})_2\text{VO}_2\text{Li}$  was obtained from  $^{18}\text{O}$ -labeled  $\text{LiH}_2\text{VO}_4$  by adding 30  $\mu\text{L}$  of 1.88 M  $\text{LiH}_2\text{VO}_4$  to 0.50 mL of anhydrous methanol (water content  $\leq 0.05\%$ , Aldrich) and allowing time for the initial precipitate to dissolve. Alternatively, dry  $(n\text{-Bu})_4\text{NH}_2\text{VO}_4$  was dissolved directly in anhydrous methanol.

**$^{16}\text{O}$ - and  $^{17}\text{O}$ -Labeled Dimeric Ethylene Glycol–Vanadate Complexes.** The  $(\text{EG}/\text{V})_2$  complex was prepared by two methods. A 2 M solution was produced by adding 2 volumes of 1.0 M  $\text{NaH}_2\text{VO}_4$  to 1 volume of ethylene glycol and removing most of the water under vacuum at 25 °C using a rotary evaporator. Additional water was removed by inserting a splash trap containing  $\text{P}_2\text{O}_5$  between the sample flask and the rotary evaporator and continuing the evaporation for 2 h at 30 °C and 1 Torr. Analysis of these solutions by  $^1\text{H}$  NMR spectroscopy showed a water content of 5% (corresponding to a  $-\text{OH}/>\text{CH}_2$  ratio of 0.585). The  $^{17}\text{O}$ -labeled  $(\text{EG}/\text{V})_2$  complex was prepared from these solutions by adding 2% (v/v) of  $[\text{^{17}O}]\text{H}_2\text{O}$  (50%) and repeating the evaporation three times to produce an  $^{17}\text{O}/^{16}\text{O}$  ratio estimated as about 0.5.

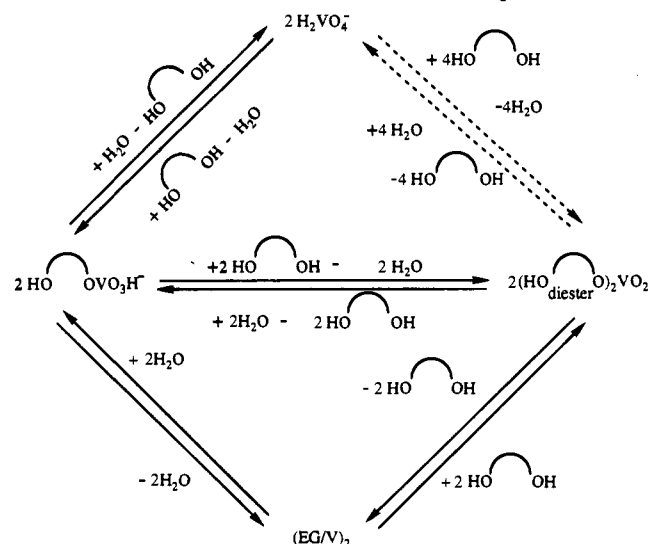
In the second procedure, 1–2 mmol of dried  $\text{LiH}_2\text{VO}_4$ ,  $(n\text{-Bu})_4\text{NH}_2\text{VO}_4$  or  $(\text{CH}_3)_4\text{NH}_2\text{VO}_4$  was dissolved directly in anhydrous ethylene glycol by stirring for several hours under  $\text{N}_2$ , shielded from direct light. If necessary, the small amount of undissolved solid was removed by centrifugation. In some cases, the solutions were dried with an excess of  $\text{CaSO}_4$  (with only minor losses of vanadate). To obtain the  $^{17}\text{O}$ -labeled  $(\text{EG}/\text{V})_2$  solutions were prepared by adding  $[\text{^{17}O}]\text{H}_2\text{O}$  (50%) to ethylene glycol.

**Dimeric  $\beta$ -Methyl Riboside–Vanadate Complex ( $\beta\text{MR}/\text{V})_2$  and Dimeric Adenosine–Vanadate Complex.** The  $(\beta\text{MR}/\text{V})_2$  was obtained by mixing stock solutions of  $\beta$ -methyl riboside (Sigma) and the  $\text{Na}^+$  or  $\text{Li}^+$  salt of  $\text{H}_2\text{VO}_4^-$  in  $\text{D}_2\text{O}$  (Cambridge), previously demetalated by passage through a column of a mixed cation–anion resin (AG-501, BioRad). The solution containing 0.30 M  $\beta$ -methyl riboside and 0.20 M  $\text{H}_2\text{VO}_4^-$  (or 0.45 M of both) was subjected to two freeze–thaw cycles under vacuum before being stored under vacuum in the dark. The adenosine complex was obtained similarly, except that the solutions were prepared in containers previously soaked in dilute EDTA and rinsed thoroughly with doubly-distilled water before use; in addition, solutions of complexes were prepared under  $\text{N}_2$  and shielded from direct light. Final concentrations of adenosine and  $\text{H}_2\text{VO}_4^-$  were 43 and 25 mM, respectively. The  $^{51}\text{V}$  NMR spectra of all solutions showed a single resonance with a chemical shift about  $-523$  ppm, in agreement with previous characterization of this complex.<sup>4</sup>

**Dimeric 2-Hydroxyisobutyric Acid–Vanadate ( $\text{HiB}/\text{V})_2$  and 2-Ethyl-2-hydroxybutanoic Acid–Vanadate ( $\text{EBH}/\text{V})_2$  Complexes.** The  $(\text{HiB}/\text{V})_2$  and  $(\text{EBH}/\text{V})_2$  complexes were produced by a variation of the procedure described by Harnung *et al.*<sup>13</sup>  $\text{V}_2\text{O}_5$  (91 mg, 0.0010 M) was added to 1.00 mL of a 1.00 M solution of the  $\text{Li}^+$  (or  $\text{NH}_4^+$ ) salt of the 2-hydroxyisobutyric acid or 2-ethyl-2-hydroxybutanoic acid. The deoxygenated solutions in sealed tubes were heated at 60 °C under vacuum in the dark for 0.5 h with vigorous stirring. If necessary, traces of insoluble material were removed by centrifugation, and the vanadate concentration was determined as described above.  $^{51}\text{V}$  NMR spectra showed that more than 95% of the vanadium in such solutions was present as  $(\text{HiB}/\text{V})_2$  (at  $-551$  ppm) or  $(\text{EBH}/\text{V})_2$  (at  $-548$  ppm). These solutions were used for vibrational spectroscopy without further manipulation. Crystals of both the  $\text{Li}^+$  and  $\text{NH}_4^+$  salts of the  $(\text{EBH}/\text{V})_2$  complex for solid phase vibrational spectroscopy were obtained after cooling the respective solutions to 0 °C. The  $^{18}\text{O}$ -labeled complexes were prepared by dissolving the solid compound in  $>100$ -fold of  $[\text{^{18}O}]\text{H}_2\text{O}$ , evaporation, and repetition of this process once before dissolution in  $[\text{^{18}O}]\text{H}_2\text{O}$ .

**Spectroscopic Studies.**  $^{51}\text{V}$  NMR spectra were recorded at room temperature with a Varian VXR 500 NMR spectrometer operated at

### Scheme 1. Proposed Stoichiometric Relationship for Formation and Hydrolysis of the $(\text{EG}/\text{V})_2$ Complex



131.4 MHz or a modified Bruker AC-300P NMR spectrometer. Spectra were recorded in the unlocked mode with an acquisition time of 0.06 s, a relaxation delay of 0.15 s, and a flip angle of 42°. The chemical shift of a 0.5 M solution of vanadate in 2 M NaOH ( $\text{VO}_4^{3-}$ ,  $-541.2$  ppm)<sup>23</sup> was used as an external reference. The free induction decay was transformed using a line broadening factor of 20 Hz. The concentrations of vanadium(V) species were calculated from the mole fractions of respective vanadium species as described previously.<sup>13</sup>  $^1\text{H}$  and  $^{13}\text{C}$  NMR spectra were obtained with the same instrument operated at 499.8 and 125.7 MHz, respectively. A  $\text{D}_2\text{O}$  lock was used along with acquisition times, relaxation delays, flip angles, and line broadening factors of 2 s, 1 s, 1.2°, and 0.5 Hz for  $^1\text{H}$  and 3 s, 3 s, 60°, and 15 Hz for  $^{13}\text{C}$ . Chemical shifts for  $^1\text{H}$  and  $^{13}\text{C}$  are reported relative to TMS. Chemical exchange rates for the anomeric protons of the isomeric  $(\beta\text{MR}/\text{V})_2$  complexes were measured using the methods and parameters described previously.<sup>24</sup>  $^{17}\text{O}$  NMR spectra were recorded at 40.7 MHz (7.0 T) on a modified Bruker AC-300P MHz spectrometer in unlocked mode. A temperature of 298 K was used with spectral widths from 17 857 to 100 000 Hz, a 90° pulsewidth, a 4 ms acquisition time, and a 0.07 ms relaxation delay. Chemical shifts are recorded with respect to  $[\text{^{17}O}]\text{H}_2\text{O}$ .

Raman difference spectra were obtained as described by Ray *et al.*<sup>25</sup> Fourier transform infrared difference spectra were obtained with a Perkin-Elmer Model 1600 FTIR spectrometer. Scans, at 2  $\text{cm}^{-1}$  resolution, of solutions with and without added  $\text{H}_2\text{VO}_4^-$  salt were collected in the ratio mode. The resulting spectra were subtracted from each other, digitally, and the difference converted to absorbance.

**Bond Strength Calculations.** When possible, vanadium–oxygen bond strengths,  $s_{\text{VO}}$ , are calculated from reported bond lengths,  $l$  (expressed in Å units), as described in eq 2,<sup>26</sup> and expressed in terms of valence units per bond,  $\text{vu}$ .<sup>25</sup> Alternatively,  $s_{\text{VO}}$  can be calculated from the symmetrical stretching frequencies,  $\nu_s$ , as described in eq 3,<sup>25</sup>

$$s_{\text{VO}} = (l/1.791)^{-5.1} \quad (2)$$

$$s_{\text{VO}} = [0.300 \ln(20\,000/\nu_s)]^{-5.1} \quad (3)$$

## Results and Discussion

In view of the diverse nature of the studies reported herein, data that support the stoichiometries shown in Scheme 1 are described first. Second, spectroscopic data are presented that lead to a new structural proposal for the  $(\text{EG}/\text{V})_2$  complex.

(23) Howarth, O. W. *Prog. NMR Spectrosc.* **1990**, *22*, 453–483.

(24) Post, C. B.; Ray, W. J., Jr.; Gorenstein, D. G. *Biochemistry* **1989**, *28*, 548–558.

(25) Ray, W. J., Jr.; Burgner, J. W., II; Deng, H.; Callender, R. *Biochemistry* **1993**, *32*, 12977–12983.

(26) Brown, I. D.; Wu, K. K. *Acta Crystallogr.* **1976**, *B32*, 1957–1959.

**Table 1.** Formation of the (EG/V)<sub>2</sub> Complex from the Corresponding Diester in Ethylene Glycol as Determined by <sup>51</sup>V NMR Spectroscopy<sup>a</sup>

total LiH <sub>2</sub> VO <sub>4</sub> (mM)	diester (mM)	(EG/V) <sub>2</sub> (mM)	K <sub>4</sub> <sup>b</sup> (mM <sup>-1</sup> )	γ <sub>C</sub> <sup>±</sup> /(γ <sub>D</sub> <sup>±</sup> ) <sup>2 c</sup>
10	2.87	3.56	0.43	1.00
20	4.22	7.89	0.45	1.02
30	5.06	12.5	0.49	1.08
40	5.60	17.2	0.55	1.13

<sup>a</sup> Equilibrium assessed in commercial anhydrous ethylene glycol by <sup>51</sup>V NMR. Only two resonances were detected, those of the diester and of (EG/V)<sub>2</sub>. <sup>b</sup> The equilibrium constant for eq 4 when x = 0: K<sub>4</sub> = [(EG/V)<sub>2</sub>]/[diester]<sup>2</sup>. <sup>c</sup> Required ratio in order that K<sub>4</sub> = 0.43 mM.

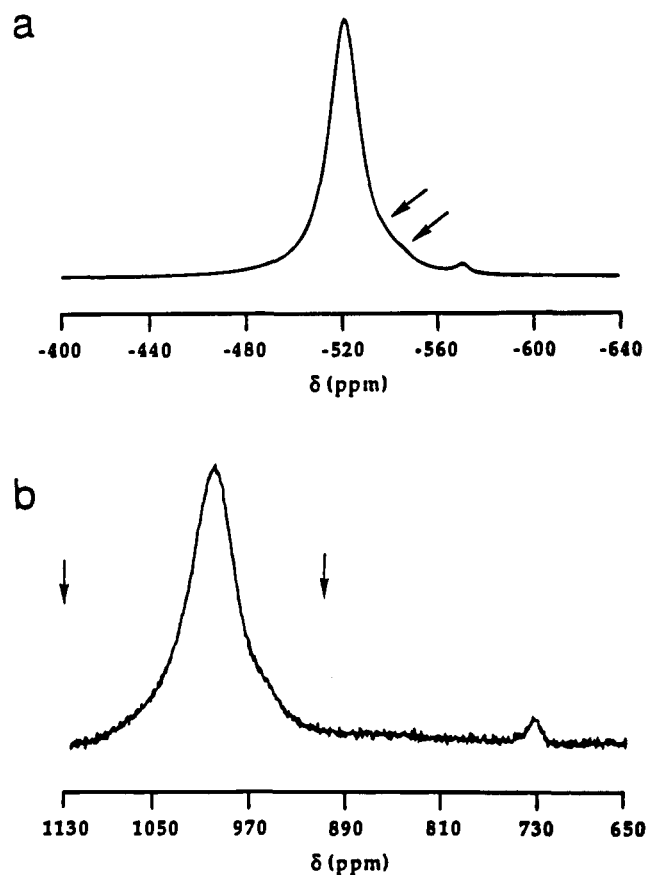


**Figure 2.** <sup>51</sup>V and <sup>17</sup>O NMR spectra of the (EG/V)<sub>2</sub> complex. A solution of 1.3 M (Me<sub>4</sub>N)H<sub>2</sub>VO<sub>4</sub> in ethylene glycol containing 10% [<sup>17</sup>O]H<sub>2</sub>O was prepared from the residue obtained from a solution of the vanadate salt after thorough drying. The <sup>51</sup>V NMR spectrum was recorded at 79 MHz (a) and the <sup>17</sup>O NMR spectrum was recorded at 40.7 Hz (b) using a modified Bruker AC-300P MHz spectrometer. Baseline corrections in the <sup>17</sup>O NMR spectrum were made by selecting a 300–400 ppm wide section of the spectrum for display on the graphics monitor, using the Expansion and Phase (EP) subroutines in the Bruker DISNMR. The K subroutine was used to make manual interactive changes in the baseline on the basis of the observed effect of polynomial corrections on the spectrum. See the text for species producing the chemical shifts indicated by arrows.

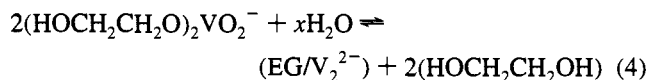
Finally, several additional lines of spectroscopic data are presented to further differentiate between the current proposal (Figure 1e) and the previous proposals (Figure 1a–d). The results of these comparisons are summarized in Table 3.

**Formation of (EG/V)<sub>2</sub> from the Monomeric Vanadate Diester: Involvement of Water.** The <sup>51</sup>V NMR spectrum of 2.0 M NaH<sub>2</sub>VO<sub>4</sub> in 94% (16.9 M) ethylene glycol–water solution (Figure 2a) contains a symmetrical resonance (full width at half-height, nearly 1800 Hz) with a chemical shift of –523 ppm. This resonance accounts for at least 95% of the vanadium present. Its full width at half-height decreases to 360 Hz in

60% (10.8 M) ethylene glycol (at 1.5 M vanadate) without a substantial change in chemical shift. The chemical shift of this resonance differs by 1.5 ppm from that reported for the (EG/V)<sub>2</sub> complex at low vanadate concentrations in 67% ethylene glycol, 20 mM Tris, and 1 M KCl.<sup>3</sup> The line width observed at 1.5 M vanadate is decreased by dilution in 60% ethylene glycol to yield the spectrum reported previously.<sup>3</sup>

Minor up-field resonances, that account for <5% of the vanadium present, were observed at –543, –554.5, and –571 ppm in the 2.0 M vanadate solution (94% ethylene glycol). The resonances at –543 and –571 ppm disappear on dilution with anhydrous ethylene glycol. Hence the species that produce these resonances are oligomeric oxovanadates. In contrast, the resonance at –554 ppm increases markedly and becomes the most prominent resonance at about 2 mM vanadate. The assignment of this species as VO<sub>2</sub>[O(CH<sub>2</sub>)<sub>2</sub>OH]<sub>2</sub><sup>–</sup> is confirmed by diluting a solution of 2 mM vanadate in ethylene glycol with water to reproduce the reported <sup>51</sup>V NMR spectrum.<sup>3</sup>

Table 1 shows the 25% change in the ratio [EG/V]<sub>2</sub>/[diester]<sup>2</sup> relative to the change in the concentrations of (EG/V)<sub>2</sub> and diester (by 500 and 200%, respectively) when the total NaH<sub>2</sub>VO<sub>4</sub> is increased from 10 to 40 mM. The observed change in the [EG/V]<sub>2</sub>/[diester]<sup>2</sup> ratio is equivalent to an altered ratio of activity coefficients for the diester and the dimeric complex of only 13% (Table 1). Although the Debye–Hückel limiting law<sup>27</sup> predicts that the equilibrium constant for dimerization of the anion of a 1:1 electrolyte (the diester) should not be a function of ionic strength, the concentration of a 40 mM sample is well above the concentrations where the law can be expected to hold. (The calculated effect on γ<sub>+</sub>γ<sub>–</sub> produced at 40 mM vanadate (Table 1 (I = 0.057 M)) is equivalent to that produced at an ionic strength of 0.45 M in water.) Hence, the observed change in the activity coefficients over the concentration range studied is reasonable in view of the reduced dielectric constant of ethylene glycol relative to water (40 as opposed to 80).<sup>28a</sup> These observations show that the conversion of the diester of ethylene glycol and H<sub>2</sub>VO<sub>4</sub><sup>–</sup> into the (EG/V)<sub>2</sub> complex does not involve water and that n in eq 1 is 2, alternatively, x in eq 4 is 0. If x is not equal to 0, then the removal of water would



shift the equilibrium of eq 4 in favor of the diester. This is contrary not only to the results in Table 1 but to the observation that drying such solutions with an excess of CaSO<sub>4</sub> did not significantly alter the ratio of the species in solution.

To further substantiate this conclusion, the stoichiometry of eq 4 was investigated in the presence of added water in a concentration range where Henry's law should apply. Here, the activity of ethylene glycol should be essentially constant and the activity of water proportional to its concentration,<sup>27,28b</sup> although the activities of the diester anion and the dianion of the dimeric complex need not be linearly related to the concentrations. In commercial anhydrous ethylene glycol containing 10 mM LiH<sub>2</sub>VO<sub>4</sub>, the concentration of water is estimated as ≤0.04 M on the basis of the water originally present in commercial ethylene glycol plus the water generated by formation of the diester (using K<sub>4</sub> = 0.43 mM<sup>-1</sup> (Table 1)).

(27) Eisenberg, D.; Crothers, D. *Physical Chemistry*; Eisenberg, D., Crothers, D., Eds.; Benjamin Cummings: Reading, PA, 1979; Chapters 7 and 8.

(28) (a) Timmermans, J. *The Physico-Chemical Constants of Binary Systems in Concentrated Solutions*; Interscience: New York, 1959; p 247. (b) Trimble, H. M.; Potts, W. *Ind. Eng. Chem.* **1935**, *27*, 66–68.

(29) Wilson, E. B., Jr.; Decius, J. C.; Cross, P. C. *Molecular Vibrations*; McGraw-Hill: New York, 1955; pp 182–193.

Under the same conditions, but when the concentration of water is increased by 6-fold (to 0.24 M), there is no significant change in  $K_4$  ( $0.44 \text{ mM}^{-1}$ ). This invariance of  $K_4$  confirms the absence of a stoichiometric involvement of water in eq 4. Although a further 2-fold increase in added water also failed to significantly change  $K_4$  (measured value,  $0.44 \text{ mM}^{-1}$ ), higher water concentrations did increase this value (at 2.8 M water (5%),  $K_4 = 0.50 \text{ mM}^{-1}$ ; at 11 M water (20%),  $K_4 = 1.06 \text{ mM}^{-1}$ ). The latter value approximates the  $K_4$  of  $1.2 \text{ mM}^{-1}$  calculated with the data reported previously<sup>3</sup> in solutions containing 67% ethylene glycol, 0.5 mM total vanadate, 20 mM Tris, and 1 M KCl. In any event, the 2.4-fold change in equilibrium constant that we observe is far less than the nearly 300-fold overall increase in  $[\text{H}_2\text{O}]$  and the increase of approximately 700-fold in  $a(\text{H}_2\text{O})$  over the above range. (The activity coefficient of water in ethylene glycol increases from about 0.36 to 0.92 over the concentration range of 1–20% water.<sup>28b</sup>) Since increased water concentration favors the  $(\text{EG}/\text{V})_2$  dianion and the addition of nonpolar solvents favors the diester monoanion (data not shown), the change in  $K_4$  at the higher water concentrations probably is a general solvent effect. Accordingly, our conclusion that the equilibrium between the ethylene glycol diester of  $\text{H}_2\text{VO}_4^-$  and the dimeric ethylene glycol–vanadate complex does not depend on  $a(\text{H}_2\text{O})$  under these conditions rests on firm grounds. In other words eq 4 is valid only when  $x = 0$  (see Scheme 1). Hence, the dimer cannot be represented by any of the previously proposed structures (1a–1c).

**Formation of  $(\text{EG}/\text{V})_2$  from the Simple Vanadate Diester: Previous Studies.** Gresser and Tracey<sup>3</sup> concluded that formation of the  $(\text{EG}/\text{V})_2$  complex from the two molecules of  $\text{HOCH}_2\text{CH}_2\text{OVO}_3\text{H}^-$  is accompanied by the elimination of one molecular of water. In contrast, the results obtained here with  $(\text{HOCH}_2\text{CH}_2\text{O})_2\text{VO}_2^-$  show that the elimination of two water molecules should occur (Scheme 1). Recently, Harnung *et al.*<sup>13</sup> concluded that Gresser and Tracey's data are consistent with the elimination of two water molecules when  $a(\text{H}_2\text{O})$  instead of  $[\text{H}_2\text{O}]$  is used in analyzing the Gresser–Tracey data. However, on the basis of MCD spectroscopy of vanadate solutions and comparisons of  $^{51}\text{V}$  NMR chemical shifts, these authors also concluded that both the monoester of ethylene glycol and  $\text{H}_2\text{VO}_4^-$  are hydrated by a tightly bound molecule in the inner sphere of the vanadium. That is,  $\text{H}_2\text{VO}_4^-$  is actually  $\text{H}_4\text{VO}_5^-$  and  $\text{ROVO}_3\text{H}^-$  is  $\text{ROVO}_4\text{H}_3^-$ . These deductions could be correct if the structure of  $(\text{EG}/\text{V})_2$  shown in Figure 1d accounted for all the protons. However, if the esters of ethylene glycol and  $\text{H}_2\text{VO}_4^-$  are hydrated in aqueous solution, the reaction stoichiometry in Scheme 1 will not produce a five-coordinate  $(\text{EG}/\text{V})_2$  complex. Conversely, if the five-coordinate structure of  $(\text{EG}/\text{V})_2$  posed here is correct, the analysis of Harnung *et al.*<sup>13</sup> implying that the monoester of  $\text{H}_2\text{VO}_4^-$  is hydrated, is incorrect. That the conclusion of Harnung *et al.* concerning the hydration of the monoester is incorrect is indicated by the failure of the six-coordinate structure in Figure 1d to provide a rationale for the results obtained from any of the four different types of spectroscopic studies of  $(\text{EG}/\text{V})_2$  and for the number of isomers of  $(\beta\text{MR}/\text{V})_2$  described below.

**Raman Spectrum of the  $(\text{EG}/\text{V})_2$  Complex.** Parts a and b of Figure 3 show, respectively, the Raman spectra of 2 M  $\text{NaH}_2\text{VO}_4$  in 95% ethylene glycol before and after subtraction of the vibrational contribution of the ethylene glycol. Parts c and d of Figure 3 show, respectively, the parallel and perpendicularly polarized isotopic difference spectra obtained when the  $(\text{EG}/\text{V})_2$  in the reference solution is produced from  $^{18}\text{O}[\text{H}_2\text{VO}_4^-]$ . In this solution, complex  $(\text{EG}/\text{V})_2$  contains the O-18 label in terminal oxygen atoms. Comparison of Figure 3c,d shows that two different symmetric stretching modes for

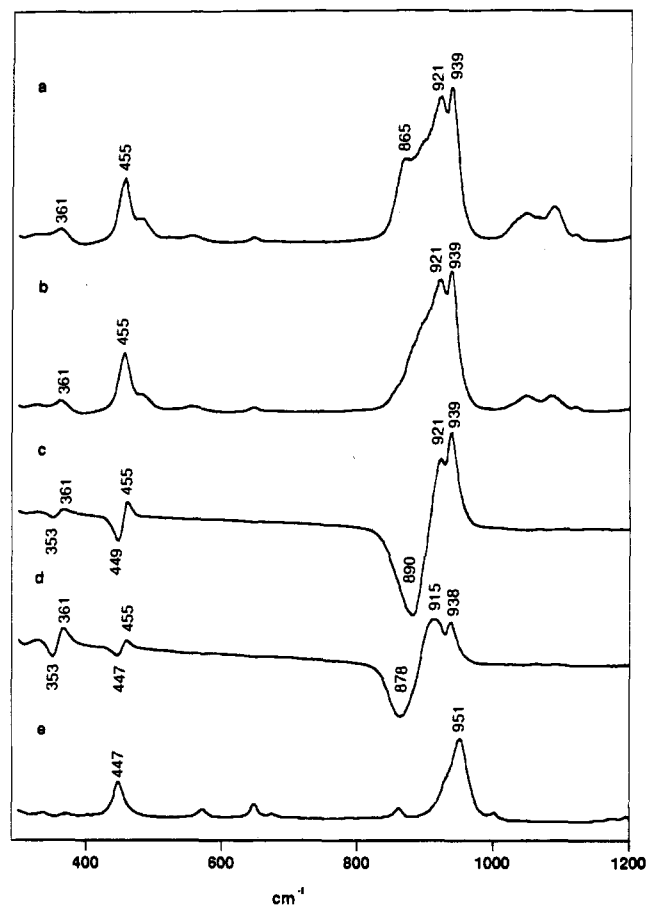


**Figure 3.** Raman spectra of the  $(\text{EG}/\text{V})_2$  and  $(\text{HiB}/\text{V})_2$  complexes. Spectra a–d were obtained with a solution that contained 2 M  $\text{NaH}_2\text{VO}_4$  in 94% ethylene glycol–water (v/v): (a) unpolarized direct spectrum; (b) the spectrum in a from which the contribution of ethylene glycol has been subtracted;  $^{16}\text{O}$ – $^{18}\text{O}$  difference spectra analogous to the spectrum in b with parallel (c) and perpendicular (d) polarization; (e) spectrum of the  $(\text{HiB}/\text{V})_2$  complex at a concentration of 0.5 M in water.

$\text{VO}$  bonds exhibit an  $^{18}\text{O}$  isotope effect: the mode that produces the split band centered at about  $930 \text{ cm}^{-1}$  and the band centered at about  $455 \text{ cm}^{-1}$ . The possible origins of these bands are considered, separately, below.

The position and shape of the split, terminal  $\text{VO}$  stretching band at about  $930 \text{ cm}^{-1}$  in the Raman spectrum of  $(\text{EG}/\text{V})_2$  (Figure 3b) are similar to those of the terminal  $\text{VO}$  stretching band of  $(\text{CH}_3\text{O})_2\text{VO}_2^-$ , at  $926 \text{ cm}^{-1}$ .<sup>14</sup> On the basis of polarization studies (Figure 3, part c vs d), the higher frequency component of the  $930 \text{ cm}^{-1}$  Raman band represents the symmetrical stretching frequency for the terminal  $\text{VO}$  in  $(\text{EG}/\text{V})_2$ . The lower frequency component arises from a more delocalized  $\text{VO}_2$  stretching mode that still is largely symmetric. A similar rationale may account for the observed band splitting of  $(\text{CH}_3\text{O})_2\text{VO}_2^-$ , where the intensity of the lower frequency component is sensitive to the identity of the counterion ( $\text{Na}^+$  as opposed to  $(\text{CH}_3)_4\text{N}^+$ ) and thus represents a stretching mode that differs fundamentally from the higher frequency mode. In any case, the vanadium atoms in  $(\text{EG}/\text{V})_2$  must be bonded to terminal oxygen atoms with bond strengths of about 1.55 vu (calculated from the higher frequency component of the band in question) that are essentially the same as those in  $(\text{CH}_3\text{O})_2\text{VO}_2^-$ . That the  $930 \text{ cm}^{-1}$  Raman band does indeed arise from terminal  $\text{VO}$  bonds is shown by the  $50 \text{ cm}^{-1}$  isotopic shift in the spectrum of  $(\text{EG}/\text{V})_2$  prepared from  $^{18}\text{O}[\text{H}_2\text{VO}_4^-]$  (Figure 3c). The absence of an apparent splitting in the  $^{18}\text{O}$  spectrum suggests that both components of the split band in the  $^{16}\text{O}$  complex have moved to lower frequencies and are either

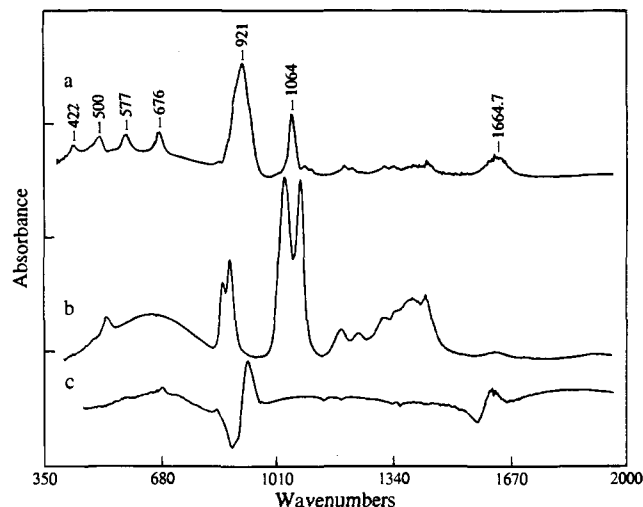


**Figure 4.** Infrared absorption spectra of the  $(EG/V)_2$  complex and related spectra: (a) the spectrum of 2 M  $NaH_2VO_4$  in 94% ethylene glycol-water minus the ethylene glycol spectrum (primary spectra scaled before subtraction by using solvent bands in the 1150–1250  $cm^{-1}$  region); (b) the spectrum of ethylene glycol that was subtracted to give a; (c) the difference spectrum of the  $(HiB/V)_2$  complex in  $[^{16}O]H_2O$  and  $[^{18}O]H_2O$ . Absorbance units (equal to 0.4) are indicated on the left-hand axis.

broadened sufficiently to mask splitting or exhibit compensating isotopic effects. These observations, coupled with the fact that there is no proton release when  $H_2VO_4^{2-}$  is converted into  $(EG/V)_2$ , are inconsistent with any of the previously proposed structures for the  $(EG/V)_2$  complex (Figures 1a–d) since, together, they show that  $(EG/V)_2$  must contain  $>V<O_0(-)$ , rather than  $>V<O_0(-)$  or  $>V<O_0(-)$  groups.

Equation 3 can be used to support the suggestion that the strength of other V–O bonds in the  $V_2O_2$  unit is significantly less than 1 vu; the 455  $cm^{-1}$  band gives rise to a calculated 0.5 vu, although the coupling of vibrational modes that can occur with bridging as opposed to nonbridging oxygens precludes a firm conclusion. However, the 455  $cm^{-1}$  band does arise from a symmetric mode (Figure 3, part c vs d) and is absent in the IR spectrum, as would be expected if this band is produced by a “breathing mode” for the  $V_2O_2$  unit. Although neither of the oxygens in the  $V_2O_2$  unit would be labeled when  $(EG/V)_2$  is prepared from  $[^{18}O]H_2VO_4^-$ , the 455  $cm^{-1}$  band exhibits a modest 6–8  $cm^{-1}$  isotope effect (Figure 3c). This isotope effect is consistent with a highly delocalized normal mode influenced by the motion of the labeled nonbridging oxygen atoms.<sup>29</sup> Although connectivities in inorganic molecules usually are represented by solid lines, regardless of bond strength, we use broken lines to represent bonds whose bond strengths are substantially less than 1 vu in the  $V_2O_2$  unit of  $(EG/V)_2$  and related structures (Figure 1).

Another aspect of the spectrum in Figure 3a is the absence of a symmetric  $-CH_2O-V-OCH_2-$  stretching mode. Although this mode is an internal mode, whose precise frequency is difficult to predict,<sup>25</sup> in  $(CH_3O)_2VO_2^-$ , it produces a broad band at about 590  $cm^{-1}$ . The absence of such a band in the spectrum of  $(EG/V)_2$  suggests that the bond strengths of the two  $-CH_2O-$  groups coordinated to a given vanadium atom are sufficiently different that they fail to produce a symmetric stretching mode. A difference in the  $-CH_2O-V-OCH_2-$  groups of both vanadiums in  $(EG/V)_2$  also is in accord with the structure proposed here (Figure 1e), but not with all the structures proposed previously.

The IR spectrum of  $(EG/V)_2$  contains a prominent band at 917  $cm^{-1}$ . This band can be seen both in a direct IR difference spectrum (Figure 4a) and in the peak/valley pattern of a  $^{16}O-$

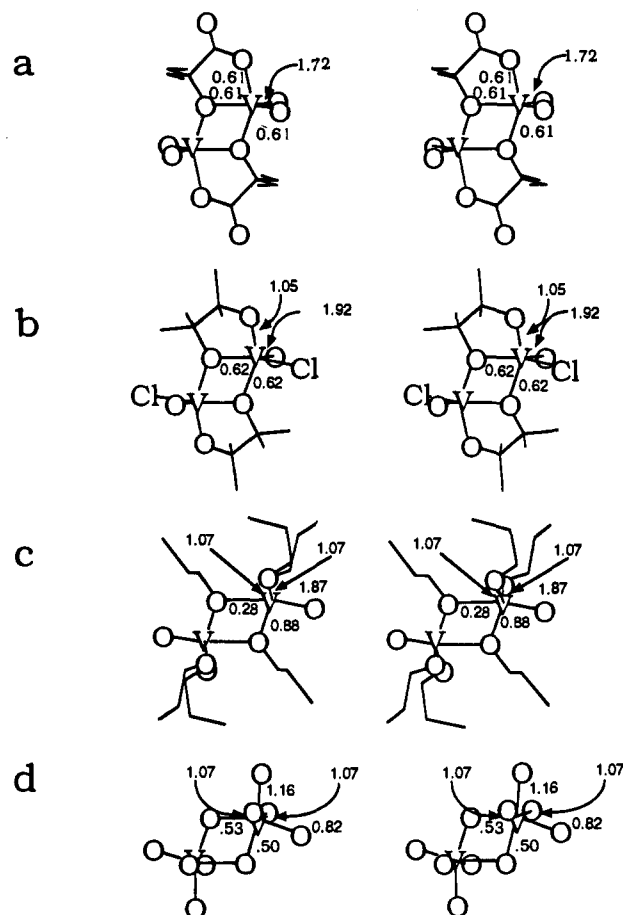


**Figure 5.** Stereographic stick-model structures of crystalline vanadate complexes containing  $V_2O_2$  units: (a) the  $(EHB/V)_2$  complex;<sup>16</sup> (b) the  $(PCI/V)_2$  complex;<sup>31</sup> (c) the crystalline dimer of tris(2-chloroethyl) vanadate;<sup>34</sup> (d) part of the lattice of trimethyl vanadate.<sup>35</sup> Estimated bond strengths from the Brown and Wu distance relationship (eq 2)<sup>26</sup> are indicated; relative bond lengths are represented by showing the structures on the same scale.

$^{18}O$  IR difference spectrum (Figure 4b). The change in frequency on isotopic substitution is about 50  $cm^{-1}$  for this band. Hence, the IR band at 917  $cm^{-1}$  likely arises from the antisymmetric stretching frequency of the  $>V<O_0(-)$  group. This rationale is consistent with that described above, since the antisymmetric stretching mode occurs at a somewhat lower frequency than the symmetric mode for vanadates.<sup>30</sup> Other IR active bands for  $(EG/V)_2$  are found at 435, 500, 574, and 672  $cm^{-1}$ .

**Proposed Solution Structure for the  $(EG/V)_2$  Complex (Figure 1e).** The only solution structure consistent with the data presented here for the  $(EG/V)_2$  complex is shown in Figure 1e. Precedence for this structure includes the known X-ray structures of related compounds: the dimeric 2-ethyl-2-hydroxybutyric acid–vanadate complex,  $(EHB/V)_2$ ,<sup>16</sup> and the dimeric pinacol– $VOCl_3$  complex,  $(P/VCl)_2$ ,<sup>31</sup> respectively. The structure for the  $(EG/V)_2$  complex (Figure 1e) differs from that of  $(EHB/V)_2$  by containing a  $-CH_2O-$  group in place of a  $-COO-$  group (Figure 5a) and from that of  $(P/VCl)_2$  by containing a  $-O^-$  in place of a  $-Cl$  (Figure 5b). Although these substitutions produce minor perturbations in the structures of the complex, both types of ligand substitutions have allowed characterization of the 2:2 complexes by X-ray crystallography when the parent compound (such as  $(EG/V)_2$ ) has been

(30) Campbell, N. J.; Flanagan, J.; Griffith, W. P. *J. Chem. Phys.* **1985**, *83*, 3712–3713.

(31) Crans, D. C.; Felty, R. A.; Miller, M. M. *J. Am. Chem. Soc.* **1991**, *113*, 265–269.

elusive.<sup>16,31–33</sup> Weak bonding between monomers in a  $V_2O_2$  unit in all of these complexes is also observed in other compounds, e.g., in tris(2-chloroethyl) vanadate<sup>34</sup> and in trimethyl vanadate<sup>35</sup> (Figure 5c,d). In the following sections, comparisons are made between solutions of  $(EG/V)_2$  and these above complexes. However, the properties of these compounds in the solid state and solutions are discussed first.

The model systems  $(EHB/V)_2$  and  $(P/VCl)_2$  are important in this study because the solution properties of these complexes have been characterized by  $^1H$ ,  $^{13}C$ , and  $^{51}V$  NMR spectroscopy and the dimeric nature of the solution structure similar to the solid-state structure has been established.<sup>13,31</sup> Similar studies have been carried out for related dimeric 2-hydroxyisobutyric acid–vanadate complex,  $(HiB/V)_2$ .<sup>13</sup> Since no structural information is available for the solid state of  $EG/V_2$ , the above compounds can be used to characterize the solution structure of  $(EG/V)_2$  by comparison. Thus, the subtle differences between the bonding within  $>VO_2^-$  groups of the  $(EHB/V)_2$  and  $(P/VCl)_2$  complexes are considered in detail below.

**Comparison of the Raman and IR Spectra of the  $(EG/V)_2$  Complex with the  $(EHB/V)_2$  and  $(HiB/V)_2$  Complexes.** Figure 3e shows the Raman spectrum of  $(HiB/V)_2$  in the region that includes the stretching frequencies of terminal VO in simple vanadates. As in the case of  $(EG/V)_2$ , there is a symmetrical stretching mode at  $951\text{ cm}^{-1}$  that shifts by about  $40\text{ cm}^{-1}$  to a lower frequency when the complex is prepared from  $[^{18}O]H_2VO_4^-$  (data not shown). Furthermore, the properties of the low-frequency band at  $447\text{ cm}^{-1}$  are similar to those of the  $455\text{ cm}^{-1}$  band of  $(EG/V)_2$ , which probably represents the breathing mode for a  $V_2O_2$  unit. Thus, both bands arise from symmetrical stretching modes. Analogous results were obtained with unlabeled  $(EHB/V)_2$ .

Figure 4b,c shows the isotopic IR difference spectra of  $(HiB/V)_2$ . Although the bands in the  $420\text{--}850\text{ cm}^{-1}$  region are much less intense than in the spectrum of  $(EG/V)_2$  (Figure 4a), these spectra and those in Figure 3 support the argument that  $(EG/V)_2$ ,  $(HiB/V)_2$ , and  $(EHB/V)_2$  contain the same basic structural unit.

**Nature of the  $VO_2$  Group in Different Bonding Arrangements.** The preceding results are consistent with the interpretation that the  $(EG/V)_2$  complex is organized about two  $>V<O_0^-$  groups. Since the Raman stretching frequency of the  $>V<O_0^-$  group in the  $(EHB/V)_2$  complexes also occurs at nearly the same frequency, both in solution and in the solid state (not shown). The terminal VO bonds in crystalline  $(EHB/V)_2$  (Figure 4c) are somewhat shorter and stronger than expected on the basis that the summed bond strengths for vanadium(5+) should be 5.0. However, the increased strength is not reflected in the VO bond frequencies of the related  $(HiB/V)_2$  complex (Figure 4c). Using the bond length/bond strength relationship for VO bonds<sup>26</sup> and the bond strength/stretching frequency relationship for vanadates,<sup>36</sup> a stretching frequency of  $970\text{ cm}^{-1}$  (corresponding to a strength of 1.7 vu) is expected for these terminal VO groups. The observed frequency is only  $951\text{ cm}^{-1}$  in solution and  $958\text{ cm}^{-1}$  in the solid (Figure 3e).

Although consideration of reasons for the unsatisfactory bond length/bond strength relationship for terminal VO bonds of a  $V_2O_2$  unit adjacent to carboxylates is beyond the scope of this study, we suggest the possibility that ligand–ligand interactions

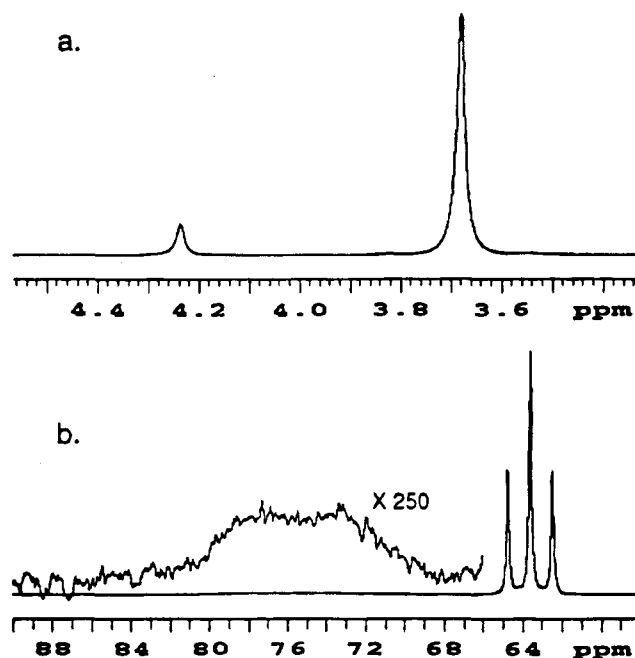


**Figure 6.**  $^1H$  and  $^{13}C$  NMR spectra of the  $(EG/V)_2$  complex: (a)  $^1H$  NMR spectrum of the 2 M complex in 90% ethylene glycol/10%  $D_2O$  (chemical shifts are 3.68 (ethylene glycol) and 4.24  $(EG/V)_2$  ppm relative to HDO = 5.7 ppm); (b)  $H^1$ -coupled  $^{13}C$  NMR spectrum of the solution used in a.

are the source of the problem. Thus, bond strengths in the  $VO_2$  group of  $VO_2(OCH_3)_2^-$ , where the ligands are alkoxides, differ substantially from those in  $VO_2^-$  complexes with oxalate or EDTA, where the corresponding ligands are carboxylates, as in  $(EHB/V)_2$  and  $(HiB/V)_2$ .<sup>18</sup> In fact, the reduced negative charge on the  $VO_2$  moiety in the EDTA-type complexes, usually represented as  $VO_2^+$ , is expected to produce a strengthening of the nonbridging terminal VO bonds relative to the terminal VO bonds in  $(CH_3O)_2VO_2^-$ , where the electrostatic charge is much more localized.

**$^1H$  and  $^{13}C$  NMR Spectra of  $(EG/V)_2$ .** The  $^1H$  NMR spectrum of  $(EG/V)_2$  (about 2 M  $(EG/V)_2$  in 90% ethylene glycol and 10%  $D_2O$ ) consists of a single, narrow resonance at a field that is lower than for the C-H protons of the ethylene glycol solvent (3.68 ppm) by 0.56 ppm (Figure 6a). The full width of the resonance at half-height is about 16 Hz, which is the same as that of the C-H protons of the solvent. At a  $(EG/V)_2$  concentration of 2 M, the integrated intensity of this resonance is about 11% of that of the ethylene glycol, as is expected from the concentration of neat ethylene glycol (18 M). Four nonequivalent protons are expected in  $(EG/V)_2$  if its structure is that shown in Figure 1b,c,e, provided these protons exchange slowly on the  $^1H$  NMR time scale (see ref 31).

The possibility that the above observation of a single  $^1H$  NMR resonance for  $(EG/V)_2$  is caused by exchange was explored using  $^{13}C$  NMR spectroscopy. The  $H^1$ -coupled  $^{13}C$  NMR spectrum of the  $(EG/V)_2$  complex at ambient temperatures contains two broad lines with chemical shifts at 73 and 78 ppm, respectively (Figure 6b). The chemical shifts of these signals are characteristic of a carbon atom coordinated to a doubly-bonded oxygen atom (73 ppm; 10 ppm shift from ethylene glycol) and a triply-bonded oxygen atom (78 ppm; 15 ppm shift from ethylene glycol).<sup>32,33</sup> Recording the  $^{13}C$  NMR spectra as a function of temperature showed that the observed signals approach coalescence as the temperature increases. The  $H^1$ -decoupled  $^{13}C$  spectra also supports the interpretation that chemical exchange occurs on the  $^{13}C$  NMR time scale (data not shown). Hence, we conclude that at ambient temperature the four protons of a given 1,2-diol unit are in rapid chemical exchange, as is

(32) Crans, D. C.; Felty, R. A.; Eckert, H.; Das, N. *Inorg. Chem.* **1994**, *33*, 2427–2438.

(33) Crans, D. C.; Marshman, R. W.; Gottlieb, M. S.; Anderson, O. P.; Miller, M. M. *Inorg. Chem.* **1992**, *31*, 4939–4949.

(34) Priebisch, W.; Rehder, D. *Inorg. Chem.* **1990**, *29*, 3013–3019.

(35) Caughlan, C. N.; Smith, H. M.; Watenpaugh, K. *Inorg. Chem.* **1966**, *5*, 2131–2134.

(36) Hardcastle, F. D.; Wachs, I. E. *J. Phys. Chem.* **1991**, *95*, 5031–5041.

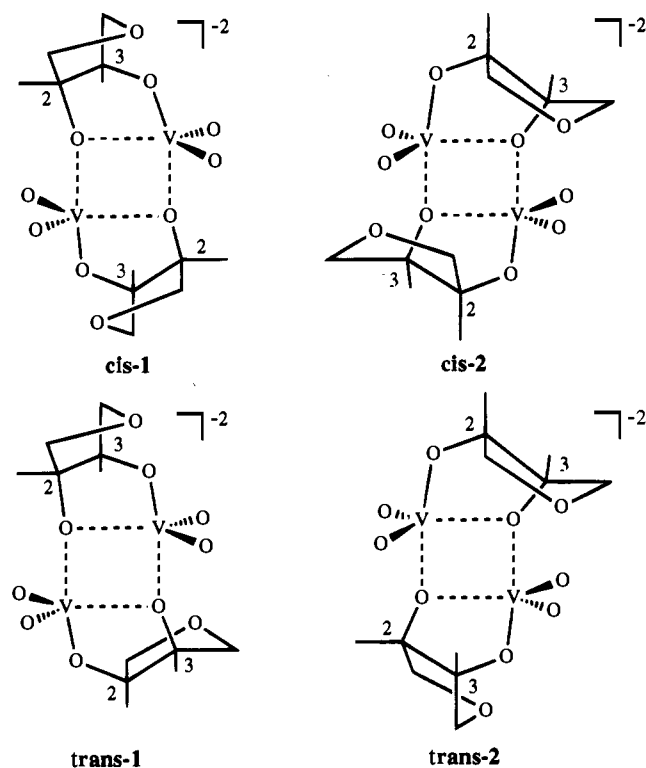


**Figure 7.** Illustration of the four possible isomers of  $(\beta\text{MR}/\text{V})_2$  that are expected on the basis of the structure in Figure 1e (the 5-methyl and 1-methoxy groups omitted for clarity). In principle, the triple-bonded oxygens are chiral, see text.

observed for the  $(\text{P}/\text{VCl})_2$  complex.<sup>31</sup> The rate constant for the process or processes that broaden the  $^{13}\text{C}$  NMR resonances of  $(\text{EG}/\text{V})_2$  is estimated as about  $1000\text{ s}^{-1}$  from the line shape in Figure 6b, by assuming that the broadening (relative to  $(\text{EHB}/\text{V})_2$ ) is caused by chemical exchange between resonances 5 ppm apart.<sup>37</sup> Since dynamic processes associated with this complex are disguising structural details in this complex, it was necessary to explore the spectroscopic properties of other  $(\text{diol}/\text{V})_2$  complexes.

#### Isomeric $(\text{Diol}/\text{V})_2$ Complexes and Their Interconversion.

The nonequivalent magnetic environments of the four pairs of methyl hydrogens in solutions of  $(\text{P}/\text{VCl})_2$  at 212 K are readily understood in terms of its crystal structure (Figure 5b).<sup>31</sup> Indeed, mixtures of vanadate plus chiral vicinal diols generate several isomers observable by  $^1\text{H}$  NMR spectroscopy.<sup>4,10</sup> For example, four structural isomers can form for the  $(\beta\text{-methyl riboside}/\text{vanadate})_2$  complex  $(\beta\text{MR}/\text{V})_2$ . In two of these, the ribose rings would be *cis* (*cis*-1 and *cis*-2); in the other two, they would be *trans* (*trans*-1 and *trans*-2) (Figure 7). The rigid nature of the  $\beta\text{-methyl riboside}$  should significantly slow down the dynamic processes observed by  $^{13}\text{C}$  NMR so that more than one isomer would be distinguished in a  $^1\text{H}$  NMR spectrum. However, it is unlikely that the two *trans* isomers could be distinguished since these isomers differ only because of an asymmetry around the triply-bonded oxygen atom caused by ring puckering. The observation of three isomeric  $(\text{diol}/\text{V})_2$  complexes thus would provide support for the proposed structure of  $(\text{EG}/\text{V})_2$ .

In fact, four resonances are observed for each proton of the ribose ring in the  $^1\text{H}$  NMR spectrum of the isomeric  $(\beta\text{MR}/\text{V})_2$  complexes (Figure 8 and Table 2): one each for the two *cis* isomers and two for the *trans* isomer. As shown in Figure 7, in one *cis* dimer, the C(2) atoms of two identical ribose rings would be adjacent to a triply-bonded oxygen and lie on the same

face of the  $\text{V}_2\text{O}_2$  unit; in the other, the C(3) atoms of both rings would be so positioned. In the *trans* dimers, the opposite halves of the molecule would be related to one or the other of two *cis* isomers. In discussing the relationship of the four anomeric proton resonances of  $(\beta\text{MR}/\text{V})_2$  to the structure in Figure 1e, we label those resonances a, c, b, and f, as in the adenosine complex  $(\text{adenosine}/\text{V})_2$ .<sup>10</sup> Thus, resonances a and c represent the two *cis* isomers, whereas the *trans* isomer is represented by two resonances, b and f. The relative integrated intensities for these resonances, at 4.58, 4.37, 4.63, and 4.26 ppm, respectively, are approximately 2.7:1.8:1:1; hence, the ratio *cis*-1:*cis*-2:*trans* is 2.7:1.8:2.0.

Saturation transfer experiments using  $(\beta\text{MR}/\text{V})_2$  show the following chemical exchange relationships between the two pairs of resonances a/c (eq 5) and b/f (eq 6). The measured values of

$$a \xrightleftharpoons[k_c]{k_a} c \quad (5)$$

$$b \xrightleftharpoons[k_f]{k_b} f \quad (6)$$

$k_a$ ,  $k_c$ ,  $k_b$ , and  $k_f$  for  $(\beta\text{MR}/\text{V})_2$  are 2.5, 3.5, 5.8, and  $5.8\text{ s}^{-1}$ , respectively. The time constant for conversion of either of the *cis* isomers, a or c, into the *trans* isomer, b plus f, is at least 10 s and could not be assessed accurately because  $T_1 \approx 1\text{ s}$ . As in the case of  $(\text{adenosine}/\text{V})_2$ , the time constant for interconversion of the two *cis* isomers ( $k_a$  and  $k_c$ ) is significantly longer than the time constant for chemical exchange between the two ribose units of the *trans* isomer ( $k_b$  and  $k_f$ ). Combined, these data suggest that the interconversion of the two *cis* isomers or the two ribose rings of the *trans* isomer involves a low-energy process such as the elimination of the two cross-ring bridges to give macrocycle c or macrocycle t, respectively, followed by reformation of alternative cross-ring bridges (Figure 9).

Regardless of the mechanism for interconverting the various isomers of  $(\beta\text{MR}/\text{V})_2$ , a structure containing two anhydride-like bridging oxygens that are identical, such as that shown in Figure 1d, is not consistent with two resolvable *cis* isomers.<sup>12,13</sup> In addition, the structure shown in Figure 1e avoids the predicament of the models shown in Figure 1b,c, both of which fail to suggest a mechanism for this isomer interconversion that is reasonable, both physically and chemically. Only the solution structure of the type of Figure 1e that can undergo isomer interconversion along a pathway similar to that outlined in Figure 9 provides a facile rationale for all of the observations described both here and elsewhere.

The properties of a related glycol–vanadium complex support the above mechanism for interconversion of *cis* and *trans* isomers. Thus, the condensation of two molecules of triethylsilylated ethylene glycol with two molecules of  $\text{VOCl}_3$  in organic solvents produces a dimeric complex with a stoichiometry analogous to that of  $(\text{PCl}/\text{V})_2$ .<sup>38</sup> Crystallographic characterization of this ethylene glycol–vanadium(5+) 2:2 complex demonstrates that it contains four-coordinate vanadium(5+) and lacks the cross-ring interactions in the  $(\text{EG}/\text{V})_2$  and  $(\text{PCl}/\text{V})_2$  complexes. (The distance between the vanadium and pertinent oxygen atoms is 3.92 Å.) However, dissolution in organic solvents produces two complexes, one of which is the 10-membered ring observed in solid state and the other a  $(\text{PCl}/\text{V})_2$ -type structure.<sup>38</sup> There is no structural evidence for such a 10-membered ring in aqueous solutions of  $(\beta\text{MR}/\text{V})_2$  or  $(\text{EG}/\text{V})_2$  or other  $(\text{diol}/\text{V})_2$  complexes. However, the observed differences in the rates of isomer conversion between *cis* complexes and between a *cis* and a *trans* complex support the

(37) Ray, W. J., Jr.; Post, C. B.; Rhyu, G. I. *Biochemistry* **1993**, *32*, 48–57.

(38) Crans, D. C.; Felty, R. A.; Anderson, O. P.; Miller, M. M. *Inorg. Chem.* **1993**, *32*, 247–248.



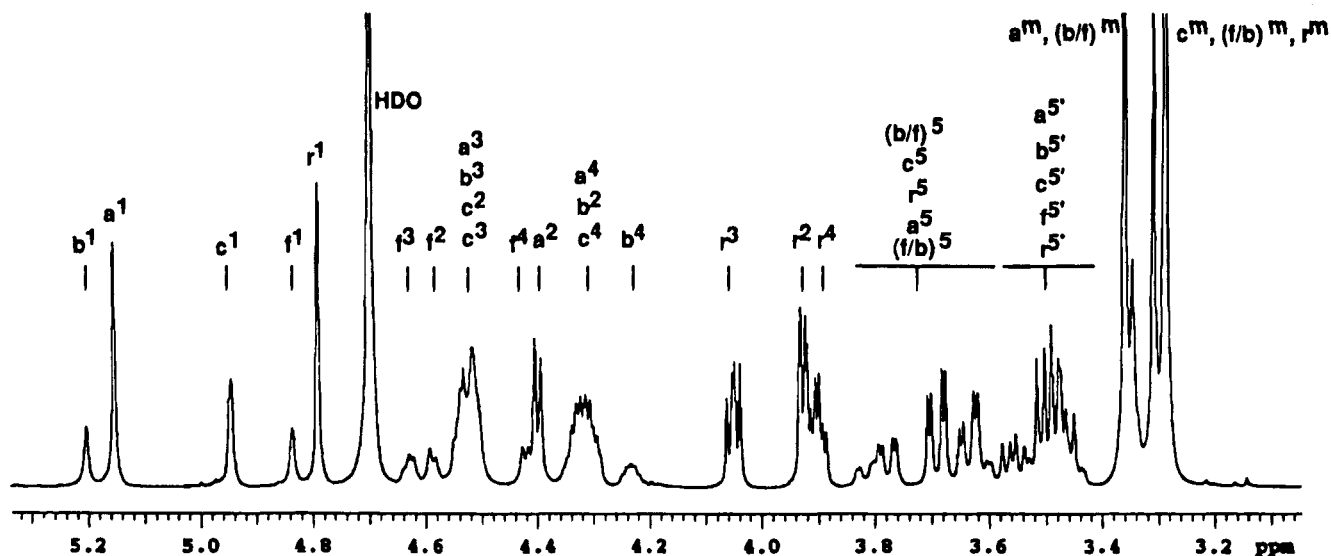


**Figure 8.**  $^1\text{H}$  NMR spectrum of the  $(\beta\text{MR}/\text{V})_2$  complex. For assignments of resonances, see Table 2. Chemical shifts are reported relative to HDO = 5.7 ppm.

**Table 2.**  $^1\text{H}$  NMR Chemical Shifts and Relative Intensities of the Resonances of  $\beta$ -Methyl Riboside and the  $(\beta$ -Methyl Riboside/ $\text{V})_2$  Complexes

resonance <sup>a</sup>	chemical shift <sup>b</sup>	rel integrated intens: obsd <sup>c</sup>	rel integrated intens: expected <sup>d</sup>
b <sup>1</sup>	5.21	2.5	
a <sup>1</sup>	5.16	7.0	
c <sup>1</sup>	4.95	4.6	25.4
f <sup>1</sup>	4.85	2.7	
r <sup>1</sup>	4.80	8.6	
f <sup>3</sup>	4.64	5.5	5.2
f <sup>2</sup>	4.60		
a <sup>3</sup> , b <sup>3</sup> , c <sup>2</sup> , c <sup>3</sup>	4.56	18.7	18.8
f <sup>4</sup> , a <sup>2</sup>	4.42	10.0	9.6
a <sup>4</sup> , b <sup>2</sup> , c <sup>4</sup>	4.33	14.7	14.2
b <sup>4</sup>	4.24	3.1	2.6
r <sup>3</sup>	4.06	8.4	8.6
r <sup>2</sup> , r <sup>4</sup>	3.93	17.0	17.2
(b/f) <sup>5</sup> , c <sup>5</sup> , r <sup>5</sup> , a <sup>5</sup> , (f/b) <sup>5</sup>	3.70	25.5	25.4
a <sup>5'</sup> , b <sup>5'</sup> , c <sup>5'</sup> , f <sup>5'</sup> , r <sup>5'</sup>	3.50	26.5	25.4
a <sup>m</sup> , (b/f) <sup>m</sup>	3.37	29.6	28.8
c <sup>m</sup> , (f/b) <sup>m</sup> , r <sup>m</sup>	3.29	49.0	47.2

<sup>a</sup> Resonances in Figure 8 are listed in order from left to right. In composite peaks, the chemical shifts of resonances not listed in alphabetical order decrease from left to right, as indicated by cross peaks in a COSY experiment performed under similar conditions. The anomeric proton resonances a<sup>1</sup>, c<sup>1</sup>, and (b<sup>1</sup> + f<sup>1</sup>) are produced by the *cis*-1, *cis*-2, and *trans* isomers and r<sup>1</sup> is produced by free  $\beta$ -methyl riboside (see ref 10). Numerical superscripts refer to the protons of the ribose unit; superscript m refers to the methyl protons. The protons of two different ribose rings of the *trans* isomer which are not distinguished, f and b, are designated b/f or f/b. <sup>b</sup> The center of composite resonance is approximated. <sup>c</sup> The sums in the right-hand portion of this column from top to bottom are for H<sup>1</sup>, H<sup>2</sup> + H<sup>3</sup> + H<sup>4</sup>, H<sup>5</sup>, and H<sup>m</sup>, respectively. <sup>d</sup> Expected integrated intensities based on the assignments in column 1 and the integrated intensities for the anomeric protons in column 3.

interpretation that a dynamic process analogous to that described above also occurs in aqueous solution. Hence, all of our NMR studies are satisfactorily explained if Figure 1e represents the structure of  $(\text{EG}/\text{V})_2$ .

The  $^1\text{H}$  NMR spectrum of the  $(\text{adenosine}/\text{V})_2$  complex contains four major but, in addition, also contains at least four minor anomeric proton resonances,<sup>11</sup> even when the complex is prepared under nitrogen and light is excluded. The origin of the major isomers undoubtedly is analogous to those suggested for  $(\beta\text{MR}/\text{V})_2$ , whereas the major/minor isomer pairs might correspond to *synlant* isomers.

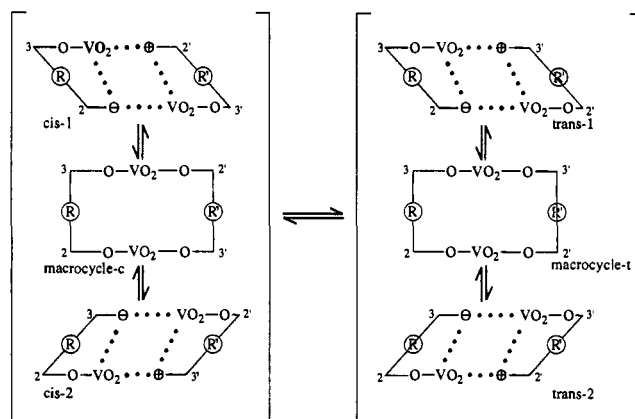


**Figure 9.** Schematic illustration of possible isomer interconversion for  $(\beta\text{MR}/\text{V})_2$  complexes. The relationship between the C(2) and C(3) atoms of the two ribose rings is indicated. The view is approximately 90° clockwise from that in Figure 7. The two *trans* isomers differ in terms of the spatial arrangement of groups about the triply-bonded oxygens, designated as  $\oplus$  and  $\ominus$ , although different  $^1\text{H}$  NMR signals are not expected.

**$^{17}\text{O}$  NMR Studies of the  $(\text{EG}/\text{V})_2$  Complex.** Oxygen-17 NMR spectroscopy is a powerful tool for exploring the structure of oxometalates. It is particularly suited to a critical evaluation of the structures that have been posed for the  $(\text{EG}/\text{V})_2$  complex because the  $^{17}\text{O}$  NMR chemical shift is sensitive to differences in metal-oxygen bond strength.<sup>39,40</sup> Specifically,  $^{17}\text{O}$  NMR spectra have the potential for distinguishing between terminal (nonbridging) oxygens and bridging oxygen atoms in vanadates because the bond strengths<sup>25</sup> of these types of oxygen atoms differ.

Figure 2b shows the  $^{17}\text{O}$  NMR spectrum of  $(\text{EG}/\text{V})_2$  obtained with a concentrated solution of  $(\text{Me}_4\text{N})\text{H}_2\text{VO}_4$  in 90% ethylene glycol-water (50 atom %  $^{17}\text{O}$  in the water). Under these conditions, all non-ester oxygen atoms in vanadates are labeled with  $^{17}\text{O}$ , both bridging and nonbridging oxygen atoms.<sup>19</sup> The major peak in this figure, with a line width of 1730 Hz (42.5 ppm) and a chemical shift of 1004 ppm, relative to  $[\text{H}_2\text{O}]^{17}\text{O}$ , accounts for more than 95% of the  $^{17}\text{O}$  NMR signals observed (exclusive of  $[\text{H}_2\text{O}]^{17}\text{O}$ ). We assign the 1004 ppm resonance

(39) Klemperer, W. G.; Shum, W. *J. Am. Chem. Soc.* **1977**, *99*, 3544-3545

(40) Klemperer, W. G. *Angew. Chem., Int. Ed. Engl.* **1978**, *17*, 246-254.

to the non-ester oxygen atoms of  $(EG/V)_2$ , since more than 95% of the vanadium in the solution is in the form that produces the  $-523$  ppm signal in the  $^{51}\text{V}$  NMR spectrum of this complex (Figure 2a). In Figure 2b, a minor resonance is observed at 724 ppm. Integration of this resonance produced an intensity of only 2–3% of the major signal. Hence, the smaller resonance is produced by a different species, not by a different type of oxygen atom in  $(EG/V)_2$ . Dilution studies support an assignment of this minor resonance to the terminal oxygen atoms of vanadate dimer, as does a previous report of the chemical shift for this species.<sup>41</sup>

To interpret the above spectrum, we first consider the expected chemical shifts for the structure proposed in Figure 1e. Since there are two different terminal oxygen atoms in this structure, an important question is whether these should produce one signal or two signals in a 1:1 ratio. If the intrinsic chemical shifts of both terminal oxygen atoms in Figure 1e are similar, the resonances would be superimposed and thus consistent with the observation of only one signal. Alternatively, coalescence of signals from two different oxygen atoms could be obtained by chemical exchange on the  $^{17}\text{O}$  NMR time scale. There is precedence for both scenarios, and in the case of  $(EG/V)_2$ , both possibilities are reasonable.<sup>39,41,42</sup> In fact, dynamic processes were observed in the  $^1\text{H}$  and  $^{13}\text{C}$  NMR spectra of the  $(EG/V)_2$  complex, and although the observed processes would be slow on the  $^{17}\text{O}$  time scale, dynamic exchange cannot be excluded without further consideration. On the other hand, the following structural considerations describe our expectations with respect to the chemical shifts, regardless of exchange processes.

Assuming that  $(EG/V)_2$  contains a  $\text{V}_2\text{O}_2$  unit similar to those that have been characterized structurally, the two terminal oxygen atoms will be in equatorial positions with essentially identical VO bond lengths (*i.e.*, strengths) within the  $>\text{V} < \text{O}(-)$  group.<sup>16,31</sup> Since the three fused rings in Figure 1e would be nearly coplanar, with one of the two terminal oxygen atoms per vanadium above and one below the plane of these rings, as in  $(\text{EHB}/V)_2$  (Figure 5a,c), a difference between the magnetic environments of the terminal oxygen atoms due to any adjacent, nonbonded atoms should be small. We conclude that, at most, a small difference in intrinsic chemical shifts could occur between the terminal oxygens of  $(EG/V)_2$ .

A comparison of the chemical shift of  $^{17}\text{O}$  in the  $(EG/V)_2$  with other vanadates also supports the structure in Figure 1e. The chemical shift of terminal oxygen atoms in vanadates tends to be around 1000 ppm when the VO bond strength is similar to that in  $(EG/V)_2$ , about 1.55 vu, as estimated on the basis of Raman frequencies.<sup>25</sup> The  $^{17}\text{O}$  NMR chemical shift for four of the terminal oxygen atoms in the vanadate decamer with a bond strength of 1.74 vu (based on a bond length of 1.61 Å)<sup>43</sup> is 1150 ppm.<sup>39</sup> A bond strength of 1.9 vu (based on a bond length of 1.58 Å)<sup>44,45</sup> in the vanadate tetramer gives an  $^{17}\text{O}$  NMR chemical shift of 928 ppm.<sup>41</sup> The two arrows on either side of the major peak in Figure 2b show the positions of these chemical shifts. Hence, we conclude that the observed  $^{17}\text{O}$  NMR chemical shift for the terminal oxygen atoms in  $(EG/V)_2$  is consistent with that expected for the structure in Figure 1e.

The chemical shifts of bridging oxygen atoms in vanadate dimers, tetramers, and pentamers differ from those of the terminal oxygen atoms by at least 200 ppm.<sup>39,41</sup> Similar differences would be expected for the two types of oxygen atoms in the various structures of Figure 1. Since all of the non-ester oxygen atoms are terminal atoms, in the absence of chemical exchange, the structure in Figure 1e provides a simple rationale for the observed magnetic equivalence of all non-ester oxygen atoms of the  $(EG/V)_2$  complex. The possibility that a  $^{17}\text{O}$  resonance is not observed for a bridging ester oxygen of the types shown in Figure 1 is unlikely because bridged oxygen atoms in other oxoanions, including the three vanadate oxoanions noted above, are observed.<sup>39,41</sup>

On the other hand, one must consider the possibility that dynamic processes, either intramolecular or intermolecular, produce magnetic equivalence of all bridging and nonbridging non-ester oxygen atoms of  $(EG/V)_2$ . Besides being quite rapid, the intermolecular process required for structures in Figure 1a–d must alter the connectivity of oxygen atoms within a given complex, *i.e.*, a V–O–V linkage must be cleaved and reformed. It is unlikely that such a process would proceed at the necessary rate in 90% ethylene glycol, since water is required as a reactant in bond cleavage. In addition, the failure of chemical exchange to produce magnetic equivalence of the bridging and nonbridging oxygen atoms in compounds such as the vanadate dimer, even in water, casts additional doubt on an intermolecular process (see also ref 46). Hence, it is likely that any exchange process that produces magnetic equivalence of bridging and terminal oxygen atoms is intramolecular.

However, any intramolecular process that equilibrates all non-ester oxygen atoms in structures 1a–d will also equilibrate the two carbon atoms of the ethylene glycol unit. In fact,  $^{13}\text{C}$  NMR studies show that some dynamic process, presumably an intramolecular process, does produce partial coalescence of the resonances from these two carbon atoms (see Figure 6b), whose chemical shifts differ by several ppm. Such a process would be slow on the  $^{17}\text{O}$  NMR time scale if the chemical shift of the two types of oxygens differed by 50 ppm or more and would produce a recognizable asymmetry and/or resolved signals. The observed spectrum in Figure 2b rules out this possibility. Thus, unless the chemical shift of the non-ester bridging oxygens in structures in Figure 1a–d is unusually large, so that shifts for bridging and terminal oxygen atoms differ by less than 50 ppm, even intramolecular chemical exchange cannot account for the single, major NMR signal in Figure 2b. Hence, we again conclude that structures in Figure 1a–d are not consistent with the observed  $^{17}\text{O}$  NMR spectrum of  $(EG/V)_2$  and that only the structure Figure 1e is.

Finally, each line of experimental evidence presented above has been analyzed in terms of proposed structures in Figure 1a–e. Whether or not the observed experimental data are consistent with each proposed structure is summarized in Table 3.

#### Vanadate Derivatives as Probes of Enzymic Mechanisms.

Selected vanadate esters are potent inhibitors of ribonucleases, phosphatases, and phosphomutases. In several cases, the affinity of the vanadate ester for the enzyme has been attributed to the similarity between its structure, or a structure that it can assume, and the structure that characterizes the phosphate group in the transition states of the above reactions. If so, examining ground states of those vanadates that are very tightly bound to enzymes of the above type may provide clues about structural differences between phosphate groups in the ground and transition states. In addition, guidelines for the uses of such derivatives as mechanism-based inhibitors in studies of other enzymes can be obtained.

(41) Heath, E.; Howarth, O. W. *J. Chem. Soc., Dalton Trans.* **1981**, 1105–1110.

(42) Crans, D. C.; Shin, P. K. *J. Am. Chem. Soc.* **1994**, *116*, 1305–1315.

(43) Swallow, A. G.; Ahmed, F. R.; Barnes, W. H. *Acta Crystallogr.* **1966**, *21*, 397–405.

(44) Day, V. W.; Klemperer, W. G.; Yagasaki, A. *Chem. Lett.* **1990**, 1267–1270.

(45) Fuchs, J.; Mahjour, S.; Pickardt, J. *Angew. Chem., Int. Ed. Engl.* **1976**, *15*, 374–375.

(46) Crans, D. C.; Ehde, P. M.; Shin, P. K.; Pettersson, L. *J. Am. Chem. Soc.* **1991**, *113*, 3728–3736.

**Table 3.** Relationship between the Experimental Evidence Reported Here and Proposed Structures for the (Glycol/V)<sub>2</sub> Complex<sup>a</sup>

	stoichiometry	Raman spectroscopy	structural precedence	IR spectroscopic studies	isomer count	dynamic processes ( <sup>1</sup> H and <sup>13</sup> C spectroscopy)	<sup>17</sup> O NMR spectroscopy
1a	no	no	no	no	no	no	no
1b	no	no	no	no	yes	no	no
1c	no	no	indirect	no	yes	no	no
1d	perhaps <sup>b</sup>	no	no	no	no	no	no
1e	yes	yes	yes	yes	yes	yes	yes

<sup>a</sup> Whether or not the structures in Figure 1 provide a rationale for the observation reported herein is indicated. Rating of structures 1a–e with respect to previous observations has not been done. However, the structure in Figure 1e provides a rationale for all reproducible and appropriately interpreted experimental evidence, including previous work. <sup>b</sup> The stoichiometry would be correct if ROVO<sub>3</sub>H<sup>-</sup> is hydrated, and four protons are accommodated in this structure.

We begin by pointing out the generally accepted structural and electronic similarity between PO<sub>4</sub><sup>3-</sup> and VO<sub>4</sub><sup>3-</sup>.<sup>20,47,48</sup> This similarity diverges, successively, as one to three oxide oxygen atoms are protonated or alkylated. Nucleophilic attack at the P or V atom of the respective triesters is one example of this divergence.<sup>48–50</sup> During a nucleophilic attack, the strength of the terminal PO bond in a phosphate triester is reduced substantially. In contrast, many cases of nucleophilic attack on a vanadate triester do not significantly reduce the strength of the terminal VO bond. For example, (CH<sub>3</sub>O)<sub>3</sub>VO and (ClCH<sub>2</sub>CH<sub>2</sub>O)<sub>3</sub>VO associate in solution and in the solid state. This association produces the dimers shown in Figure 5c,d. In both cases, the strength of the terminal VO bond remains at about 2 vu, based on crystallographic data,<sup>34,35</sup> and the strength of one V–OR single bond is reduced to about 0.5 vu. A similar conclusion can be drawn about the solution structure of the dimer in Figure 5c<sup>25</sup> on the basis of the reported stretching frequency of its terminal VO bond.<sup>34</sup> In these adducts, the summed strengths of the VO bonds thus remain close to 5, as has been observed for a variety of vanadium(V) compounds.<sup>26</sup>

Cyclic diesters of phosphates and vanadates also show similar bonding patterns. Thus, the cross-ring bridges that characterize the (diol/V)<sub>2</sub> complexes described here can be considered the result of a nucleophilic attack on a RO–VO<sub>2</sub><sup>-</sup>–OR group to give [(RO–)(RO···)VO<sub>2</sub><sup>-</sup>(···OR)]<sup>2-</sup>; however, this perturbation leaves the bonds within the central VO<sub>2</sub><sup>-</sup> group largely unchanged. The stability of such adducts stands in sharp contrast to the expected instability of analogous five-coordinate phosphate adducts, particularly those that would resemble transition states for the reactions of various phosphate diesters. In fact, the tendency of vanadate derivatives to form stable adducts of this type provides some rationale for the ability of certain vanadate derivatives to mimic the presumed transition states for various reactions of phosphate esters, as described below.

One such reaction is an “S<sub>N</sub>2-like” displacement (*i.e.*, an A<sub>N</sub>D<sub>N</sub> reaction)<sup>51</sup> at the phosphorus of a phosphate diester with a good leaving group.<sup>52</sup> Here, the extent of bond breaking involving the leaving RO<sup>-</sup> group is more or less equal to and externally compensated by the extent of bond making involving the entering RO<sup>-</sup> or HO<sup>-</sup> group. Relatively minor changes in bonding within the central PO<sub>3</sub> group thus are expected. Hence, the appropriate vanadate derivative might well serve as a reasonable mimic of this type of transition state; compare b and d in Figure 10.

In an associative transition state leading to a phosphorane-like adduct, the character of the central PO<sub>3</sub><sup>-</sup> group in the

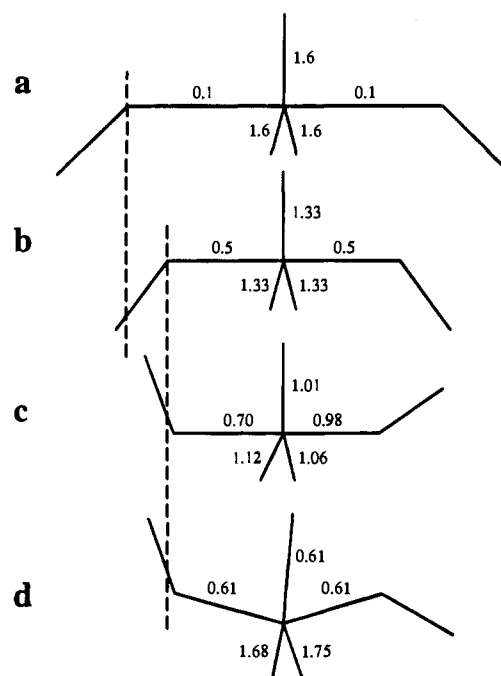


**Figure 10.** Possible transition states for PO<sub>3</sub><sup>-</sup> transfer from donor to acceptor oxygens using stick-model representations: (a) dissociative transfer of phosphate ester dianion with identical donor and acceptor oxygen atoms (bond length calculated according to Brown and Wu);<sup>26</sup> (b) transfer of phosphate ester dianion with a “S<sub>N</sub>2-like” (*i.e.*, A<sub>N</sub>D<sub>N</sub>) transition state (bond length calculated according to Brown and Wu);<sup>26</sup> (c) the PO<sub>5</sub> cluster plus attached carbons in the trisopropylphosphite phenanthrenequinone adduct;<sup>58</sup> (d) the VO<sub>5</sub><sup>-</sup> cluster of (EHB/V)<sub>2</sub>. All distances are shown on the same scale. The vertical dashed lines indicate the different P–O distances that characterize associative and S<sub>N</sub>2-type transition states.

transition state would differ substantially from that in the reactant. The bridging RO–P bonds would also be shorter than in an S<sub>N</sub>2-like transition state, perhaps by about 0.1 Å. Because of this relatively small structural difference (illustrated in b and c, Figure 10), a vanadate derivative whose structure mimicked an S<sub>N</sub>2-like transition state might well bind with substantial tenacity to an enzyme that catalyzed an associative reaction of phosphate esters. Hence, the tight binding of a vanadate derivative to an enzyme is unlikely to distinguish between active sites that are designed to facilitate S<sub>N</sub>2-like reactions, as opposed to associative reactions of a phosphate ester.

In the case of phosphate ester dianions, the transition states for all PO<sub>3</sub> transfer reactions involving compounds studied to date appear to be dissociative in nature (see ref 53 and references therein). Such transition states are characterized by weak apical P···OR bonds with strengths on the order of 0.1 vu<sup>54</sup> and strong

(47) Chasteen, N. D. *Structure and Bonding*; Clarke, M. J., *et al.*, Eds.; Springer-Verlag: New York, 1983; pp 105–138.

(48) Rehder, D. *Angew. Chem., Int. Ed. Engl.* **1991**, *30*, 148–167.

(49) Benkovic, S. J.; Schray, K. J. *Enzyme* **1973**, *8*, 201–238.

(50) White, P. J.; Kaus, M. J.; Edwards, J. O.; Reiger, P. H. *J. Chem. Soc., Chem. Commun.* **1976**, 429–430.

(51) Guthrie, R. D.; Jencks, W. P. *Acc. Chem. Res.* **1989**, *22*, 343–349.

(52) Hengge, A. C.; Cleland, W. W. *J. Am. Chem. Soc.* **1991**, *113*, 5835–5841.

(53) Herschlag, D.; Jencks, W. P. *J. Am. Chem. Soc.* **1990**, *112*, 1951–1956.

(54) Bourne, N.; Williams, A. *J. Org. Chem.* **1984**, *49*, 1200–1204.

equatorial PO bonds with strengths of up to 1.6 vu. Such strong equatorial bonds would largely compensate *internally* for the reduced strength of the bond being broken, since in a dissociative transition state bond breaking is not compensated by formation of the new bond. Although VO<sub>5</sub> constellations frequently have two long, weak VO bonds, as well as two short, strong ones, the lengths of the apical bonds in those VO<sub>5</sub> constellations that have been studied are considerably less than those of the apical PO bonds expected in a dissociative transition state for PO<sub>3</sub> transfer (compare Figure 10, parts a and c). Hence, even a carefully chosen vanadate analog seems less likely to exhibit a high affinity for an enzyme that utilizes a dissociative transition state for catalysis than one where an S<sub>N</sub>2 or associative transition state is utilized.

In phosphoglucomutase reactions, the PO<sub>3</sub> fragment of the phosphate ester dianion is surrounded by positive charges on the protein. This observation has led to the proposal of a transition state with substantially more associative character than in model reactions (Figure 10b).<sup>14</sup> In such a transition state, the strengths of the equatorial PO bonds would be similar to that for a phosphate ester dianion, 1.3 vu.<sup>25</sup> Bond breaking would be largely compensated by formation of the new P–OR bond, i.e., the strength of the new bond would be substantially greater in such an associative transition state than the strength of the corresponding bond in a dissociative transition state. As noted above, a similar arrangement of bonds is expected in a vanadate ester that is part of a VO<sub>5</sub> constellation. In accord with this expectation, a vanadate ester, Glc-1-P-6-V, that is an analog of the first product in the phosphoglucomutase reaction, Glc-1,6-P<sub>2</sub>, binds with unusual affinity to the dephospho form of phosphoglucomutase ( $K_d \approx 10^{-14}$  M).<sup>55</sup>

Substantial spectral differences between the vanadate group in the five-coordinate diol–vanadate complexes described here and the “transition-state analog complex” of phosphoglucomutase may seem inconsistent. In aqueous solution, formation of the fifth VO bond, as in the dimeric diol–vanadate complexes, shifts the most prominent near-UV band of ROVO<sub>3</sub>H<sup>−</sup> to substantially shorter wavelengths,<sup>37</sup> in accord with Lever’s paradigm, on the basis of crystal field effects.<sup>56</sup> (Longer wavelength transitions do become more prominent in such adducts, particularly in nonpolar media (W.J.R., unpublished results; see also ref 31, but here we concentrate on the most prominent near-UV band). In contrast, formation of what appears to be the fifth VO bond in the above phosphoglucomutase complex, which markedly reduces the strength of all three terminal VO bonds of the original ROVO<sub>3</sub><sup>2−</sup> ester, produces a shift of the most prominent UV band to substantially longer wavelengths.

Should a VO<sub>5</sub> cluster have a characteristic electron spin transfer spectrum in the near-UV? On the basis of the following considerations, which in turn are based on Lever’s paradigm,<sup>56</sup> we believe the answer is “No”. In Lever’s argument, formation of a long, weak fifth VO bond to a VO<sub>4</sub> constellation should increase the energy of orbitals primarily associated with the vanadium atom. Such an increase would shift the O → V electron transfer spectrum to shorter wavelengths, as observed for the diol–vanadate complexes.<sup>57</sup> The possibility that a slight weakening of the VO bonds in the original VO<sub>4</sub>, that must

accompany formation of the fifth VO bond, if the summed bond strengths are to remain at 5, would produce the opposite effect was not considered by Lever. Whereas such a weakening may not occur without external assistance to the bond-forming process, it does occur during formation of the vanadate-based transition-state analog complex of phosphoglucomutase from a VO<sub>4</sub> constellation. Accordingly, the observed red shift in the enzymatic complex can be rationalized if the energy of orbitals associated primarily with the vanadium atom are decreased more than the orbitals associated with the bond-forming process are increased. We conclude that the spectral properties of a VO<sub>5</sub> unit with bond strengths on the order of 1.5, 1.5, 0.9, 0.6, and 0.6, as might be suggested for the diol–vanadate complex on the basis of the crystal structures of related complexes,<sup>12,16</sup> are likely to differ significantly from the ones where the corresponding strengths are 1.2, 1.2, 1.2, a, and b (a + b = 1.4), as is suggested for the VO<sub>5</sub> constellation in the transition-state analog complex of phosphoglucomutase.<sup>14</sup> In spite of the five-coordinate nature of the structure proposed here for (EG/V)<sub>2</sub>, we believe that the above enzyme complex is five-coordinate, too.

### Conclusion

A variety of solution studies have been carried out to characterize the major solution complex between vanadate and vicinal glycols. Evidence based on IR, Raman, and multinuclear NMR studies is presented that rules out all previous structural proposals (see the summary in Table 3). A new structure is proposed that contains two five-coordinate vanadium atoms in VO<sub>5</sub> units within two cyclic groups of V–O–CH<sub>2</sub>–CH<sub>2</sub>–O. The geometric preferences around the vanadium atom of various vanadate esters are discussed from the standpoint of using vanadate esters as probes of enzyme mechanisms.

### Note Added in Proof

After this work was completed, we learned that Dr. Alan S. Tracey and co-workers at the Department of Chemistry, Simon Fraser University, have obtained an X-ray structure of a 2:2 vanadate–adenosine complex. The solid-state structure is analogous to that deduced from these studies (Figure 1e). In the solid-state vanadate–adenosine structure, the VO bonds in the V<sub>2</sub>O<sub>2</sub> units are 2.04 and 1.98 Å, respectively. The doubly-bonded VO bond ranges from 1.625 to 1.633 Å. Although it remains to be shown that the solid-state material has the same structure in solution, these findings support the conclusions drawn here.

**Acknowledgment.** The authors (W.J.R., J.W.B., and D.C.C.) thank the NIH for funding this work. D.C.C. also thanks the Sloan Foundation for partial funding of this work. The authors also thank Dr. Robert Callender for providing salaries for J.S. and H.D. from a grant funded by the NSF. The authors thank Dr. J. M. Puvanthingal for able technical assistance and Dr. Charles B. Roth, Department of Agronomy, Purdue University, for the use of a FTIR spectrometer. They also thank Dr. Alan Tracey, Simon Fraser University, for reading an early version of this manuscript and making a number of helpful comments.

JA943602P

(55) Ray, W. J., Jr.; Puvanthingal, J. M. *Biochemistry* **1990**, *29*, 2790–2801.

(56) Lever, A. B. *J. Chem. Educ.* **1974**, *51*, 612–616.

(57) Ray, W. J., Jr.; Post, C. B. *Biochemistry* **1990**, *29*, 2779–2789.

(58) Hamilton, W. C.; LaPlaca, S. J.; Ramirez, F.; Smith, C. P. *J. Am. Chem. Soc.* **1967**, *89*, 2268–2272.